

LOCKHEED MARTIN ENERGY RESEARCH LIBRARIES



3 4456 0451478 2

CENTRAL RESEARCH LIBRARY
DOCUMENT COLLECTION

155

ORNL-3701

C-44a - Nuclear Technology - Materials
M-3679 (35th ed.)

OAK RIDGE NATIONAL LABORATORY

STATUS AND PROGRESS REPORT

AUGUST 1964

CENTRAL RESEARCH LIBRARY
DOCUMENT COLLECTION
LIBRARY LOAN COPY
DO NOT TRANSFER TO ANOTHER PERSON
If you wish someone else to see this
document, send in name with document
and the library will arrange a loan.



OAK RIDGE NATIONAL LABORATORY

operated by

UNION CARBIDE CORPORATION

for the

U.S. ATOMIC ENERGY COMMISSION

Downgrade to Unclassified After September 4, 1965

LEGAL NOTICE

This report was prepared as an account of Government sponsored work. Neither the United States, nor the Commission, nor any person acting on behalf of the Commission:

- A. Makes any warranty or representation, expressed or implied, with respect to the accuracy, completeness, or usefulness of the information contained in this report, or that the use of any information, apparatus, method, or process disclosed in this report may not infringe privately owned rights; or
- B. Assumes any liabilities with respect to the use of, or for damages resulting from the use of any information, apparatus, method, or process disclosed in this report.

As used in the above, "person acting on behalf of the Commission" includes any employee or contractor of the Commission, or employee of such contractor, to the extent that such employee or contractor of the Commission, or employee of such contractor prepares, disseminates, or provides access to, any information pursuant to his employment or contract with the Commission, or his employment with such contractor.

ORNL-3701

Contract No. W-7405-eng-26

OAK RIDGE NATIONAL LABORATORY

STATUS AND PROGRESS REPORT

AUGUST 1964

DATE ISSUED

September 4, 1964

OAK RIDGE NATIONAL LABORATORY
Oak Ridge, Tennessee
operated by
UNION CARBIDE CORPORATION
for the
U.S. ATOMIC ENERGY COMMISSION

LOCKHEED MARTIN ENERGY RESEARCH LIBRARIES



3 4456 0451478 2

████████████████████

•

•

•

•

•

•

CONTENTS

REACTOR DEVELOPMENT.....	1
GAS-COOLED REACTOR PROGRAM.....	1
ETR Capsules.....	1
GCR-ORR Loop No. 1.....	1
LITR Capsule Irradiations.....	1
ORR Poolside Irradiations.....	1
Eight-Ball Experiment.....	2
Postirradiation Examinations of Graphite-Matrix Fuels.....	2
Instantaneous Fission-Gas Release from Coated Particles and Graphite-Matrix Fuels.....	2
Fission Product Deposition Experiment.....	2
Graphite Oxidation Experiment.....	2
Studies of Anisotropy Factors for Coated Particles and Pyrolytic Carbons.....	3
Pyrolytic-Carbon Coating Density Determinations.....	3
Heat Transfer Analysis of Fueled-Graphite Irradiation Experiments.....	3
REACTOR FUELS AND MATERIALS.....	3
Materials Compatibility Studies.....	3
Fuel Element Development.....	4
Behavior of High-Temperature Materials Under Irradiation.....	4
FUNDAMENTAL HEAT TRANSFER AND FLUID DYNAMICS.....	5
Vortex-Flow Hydromagnetic Stability Theory.....	5
Boundary-Layer Transient Phenomenon.....	5
Boiling Alkali-Metal Heat-Transfer Studies.....	5
POWER REACTOR FUEL PROCESSING.....	6
Chemical Analysis of Advanced Reactor Fuels: Determination of the Nitric Acid Oxidation Products of Carbide Fuels.....	6
Cyclic Dissolution of Irradiated Sol-Gel ThO ₂ -UO ₂	7
Batch Leaching of Irradiated ThO ₂ -UO ₂ Pellets.....	7
Pyrohydrolysis of HTGR and Coated-Particle ThC ₂ -UC ₂ Fuels.....	7
Reduction of Plutonium with Hydrogen.....	8
THORIUM UTILIZATION PROGRAM.....	8
Ultrasonic Dispersion of Carbon Black in Sols.....	8
Thorium-Uranium Fuel Cycle Development Facility.....	8
Chemistry of the Separation of Protactinium from Thorium in Molten Chloride Salts.....	9
Preparation of Sol-Gel ThO ₂ Having Controlled Porosity.....	9
Development of Equipment for Microsphere Preparation and Coating.....	9
Development of Fuel-Rod-Homogeneity Scanner.....	10
Development of Thorium-Uranium Fuel Cycle Facility Equipment.....	10
Vibratory Compaction.....	10
Completion of the Kilorod Program.....	10

Coated-Particle Development Laboratory.....	11
Irradiation of Thorium Oxide Fuels.....	11
Gas Evolution from Sol-Gel ThO ₂ -3% UO ₂	11
Extension of Sol-Gel Process to Newer Fuel Types.....	12
Permeability of Vibratorily Compacted Fuels.....	12
MOLTEN-SALT REACTOR PROGRAM.....	12
Molten-Salt Reactor Experiment.....	12
MSRE Operations.....	12
Development of Components and Systems.....	13
MSRE Pump Program.....	13
Instrument Development.....	13
NUCLEAR SAFETY.....	14
Release of Fission Products During Melting of Fuels Under Transient Reactor Conditions.....	14
Properties of Fission Product Aerosols Produced by Overheated Reactor Fuels.....	16
Behavior of Fission Products on In-Pile Destruction of Reactor Fuels.....	17
Characterization, Control, and Simulation of Accident-Released Fission Products.....	17
Nuclear Safety Information Center.....	18
Nuclear Safety Pilot Plant.....	18
RADIOACTIVE WASTE DISPOSAL.....	19
Clinch River Study.....	19
Mineral Exchange Studies.....	20
Disposal in Deep Wells.....	20
Low-Activity Waste: Pilot-Plant Work.....	20
Low-Activity Waste: Laboratory Work.....	21
Low-Activity Waste: Foam Separation.....	22
Low- and Intermediate-Activity Waste: Incorporation in Asphalt.....	23
High-Activity-Waste Solidification: Engineering Work.....	23
High-Activity-Waste Solidification: Laboratory Work.....	23
Disposal in Natural Salt Formations.....	24
Engineering, Economic, and Safety Evaluation.....	24
PHYSICAL RESEARCH.....	25
PHYSICS AND MATHEMATICS.....	25
High-Energy Physics.....	25
Physics of Fission.....	25
High-Voltage Experimental Program: Construction of a General Purpose Scattering Chamber for Charged- Particle Spectrometry.....	25
High-Voltage Experimental Program: Gamma-Ray Spectroscopy with Lithium-Drifted Germanium Detectors.....	26
Nuclear Data.....	26
Medium-Energy Nuclear Physics: Experimental.....	26
Medium-Energy Nuclear Physics: Experimental, Polarized Protons.....	27
Medium-Energy Nuclear Physics: Theory.....	27

Cyclotron Operations.....	28
Medium-Energy Electronuclear Machines.....	28
Electronuclear Systems.....	28
CHEMISTRY.....	29
Protactinium Chemistry.....	29
Transport Properties of Gases: Pressure Dependence of Thermal Diffusion.....	29
Transport Properties of Gases: Gaseous Diffusion.....	30
Analysis of Molten Salts by Electrochemical Methods: Voltammetric Measurements in Molten Fluoride Salt Systems.....	30
Spectrophotometry of Solutions over Wide Ranges of Temperature and Pressure.....	31
TRANSURANIUM-ELEMENT PRODUCTION.....	31
Chemical Process Development: Separations.....	31
Chemical Process Development: Sol Preparations.....	32
Curium Recovery Facility.....	32
Process Equipment Development: Cell Mockup.....	33
HFIR Target Fabrication Development.....	33
Transuranium Facility Design and Construction.....	33
Corrosion.....	34
METALLURGY AND MATERIALS.....	34
Research and Development on Pure Materials.....	34
Deformation in Crystalline Solids.....	35
Fundamental Research in X-Ray Diffraction.....	35
Reactions at Metal Surfaces.....	35
Spectroscopy of Ionic Media.....	36
Theory of Alloying.....	36
Fundamental Investigation of Radiation Damage in Solids: Near-Ultraviolet Luminescence in Potassium Iodide.....	37
CONTROLLED THERMONUCLEAR RESEARCH.....	37
The DCX-2 Injection-Accumulation Experiment.....	37
Active and Passive Stabilization of Plasmas and Ion Beams.....	38
Properties of Vacuum Arcs.....	38
Experimental Plasma Physics.....	39
Magnetics and Superconductivity.....	39
Vacuum Studies for Fusion.....	39
BIOLOGY AND MEDICINE.....	40
TERRESTRIAL AND FRESH-WATER ECOLOGY.....	40
Radiation Effects on Native Mammals: The Effects of Cuterebra angustifrons on the Plasma Proteins of Peromyscus leucopus.....	40
Environmental Radiation Botany: Effects of Soil Moisture on Survival of Gamma-Irradiated Pine Seedlings.....	40
Evaluation of Fission Product Distribution and Movement in White Oak Drainage System.....	41
RADIOLOGICAL PHYSICS, HEALTH PHYSICS, AND RADIATION INSTRUMENTATION.....	41

Radiation Physics and Dosimetry: An Application of the Generalized Concept of Dosimetry to Space Radiations.....	41
Radiation Physics and Dosimetry: The Application of Shell Corrections in Stopping Power to Theoretical Dose Studies.....	42
Internal Dose Estimation: Estimation of a Systemic Body Burden of Plutonium.....	42
NUCLEAR ENERGY CIVIL EFFECTS.....	42
Dosimetry and Spectrometry Research.....	42
ISOTOPE DEVELOPMENT.....	43
Stable Isotopes Development.....	43
Special Separations.....	44
Target Preparation.....	44
Radioisotope Research and Development.....	44
OPEN LITERATURE PUBLICATIONS.....	46
FOREIGN VISITORS.....	48

OAK RIDGE NATIONAL LABORATORY

STATUS AND PROGRESS REPORT

AUGUST 1964

This Status and Progress Report summarizes the unclassified portion of the Laboratory's work. Some of the topics are included every month, but the majority are reported on a bimonthly schedule.

REACTOR DEVELOPMENT

GAS-COOLED REACTOR PROGRAM

ETR Capsules. - Three EGCR-ETR capsules (E5R, E11, E12R) were discharged from the reactor July 9, completing the presently planned irradiations of EGCR-type fuel in the ETR. These capsules contained 12 hollow UO₂ pellets and had achieved estimated burnups of 6250 to 9000 Mwd per metric ton of UO₂.

GCR-ORR Loop No. 1. - Irradiation of experimental fuel assembly 14 began July 28. The fuel is a mixture of pyrolytic-carbon-coated (U,Th)O₂ particles and coated ThO₂ particles, both produced by the sol-gel process. The central temperature of the fuel reached 2170°F with no heat added to the loop coolant. Raising the coolant temperature by use of the loop heaters and by reducing the coolant flow rate brought the fuel central temperature to 2450°F, which is the maximum possible. Analysis of gas samples indicated values of the ratio of the release rate to the generation rate of approximately 1×10^{-5} for krypton isotopes.

LITR Capsule Irradiations. - Capsule L-CP9 was inserted in the LITR C-42 position on July 28 and is operating satisfactorily at indicated central fuel temperatures of 1745 to 1980°F. The capsule contains carbon-coated UC₂ particles in four separate compartments of type ATJ graphite.

ORR Poolside Irradiations. - Two capsules (O3A-6 and O4-8) containing EGCR-vendor fuel materials continued to operate at design conditions. The maximum indicated cladding temperatures are 1300 and 1540°F.

Irradiation of two sweep capsules (O5-8 and O8-8) continued; each capsule contains three 6-cm-diam fueled-graphite spheres. Capsule O5-8 has reached an estimated burnup of 1.95 at. % of the heavy metals (U + Th). The fission-gas-release rates have been increasing and are now an order of magnitude higher than the initial values. Capsule O8-8 continues to operate satisfactorily and has reached an estimated burnup of 1.04 at. % of the heavy metals (U + Th).

Operation of capsule O1-8 was terminated on July 26 when fission gases were detected in the control gas, indicating a break in a fuel can. This capsule had operated for only one ORR cycle and had reached an estimated burnup of 0.82 at. % of the heavy metals (U + Th). We had previously observed an unexplained decrease in the temperatures of spheres 1 and 2.

Eight-Ball Experiment. - The fifth eight-ball capsule (F1-8B-5) contains 1-1/2-in.-diam spheres fueled with pyrolytic-carbon-coated UC₂ and (U,Th)C₂ particles and specimens of pyrolytic-carbon-coated B₄C. The indicated central temperature for the top sphere is approximately 1800°F; the temperature of the B₄C specimens is approximately 1100°F.

Postirradiation Examinations of Graphite-Matrix Fuels. - We examined two fueled-graphite spheres, 6 cm in diameter, after irradiation. The fuel was triplex-coated (U,Th)C₂ particles; the spheres, fabricated by General Atomic, had an unfueled outer shell of type ATJ graphite. One sphere, which contained a thermocouple well in a hole drilled into the center of the sphere, was cracked. The crack originated at the central thermocouple hole and extended around the sphere to a region somewhat south of the equator; it was apparently caused by expansion of the thermocouple well.

The other sphere, similar to the first but without the thermocouple hole, appeared to be sound. Dimensional changes were less than 0.1%, except for the pole diameter, which had decreased 0.3%. A compression test on this sphere resulted in a load-to-failure of 2024 lb. There was a fair bond between the sphere core and graphite shell.

Instantaneous Fission-Gas Release from Coated Particles and Graphite-Matrix Fuels. - Experimental capsule B9-20, containing duplex-coated uranium oxide particles from batch OR-201, was irradiated for 295 hr to 4.6 at. % uranium burnup. After 172 hr (2.7% burnup) at 2200°F, a single-burst release of fission gas occurred. Six hours later there was another burst, followed by a third 35 min later. Bursts then continued at more frequent intervals as long as the temperature was held at 2200°F.

The fractional release of ⁸⁸Kr increased from 1×10^{-6} just before the first burst to 4×10^{-4} at 56 hr after the first burst. Fission-gas-release data are not complete, but based on the activity of the exit helium, it is estimated that the fractional release of ⁸⁸Kr reached 2×10^{-3} at the termination of the experiment and that 30% of the particles are broken.

Fission Product Deposition Experiment. - We are carrying out an experimental program for studying fission product transport and deposition under idealized reactor conditions. In the first series of experiments, ¹³¹I in trace amounts was injected into a flowing helium stream, and the deposition on surfaces downstream of the injection point was determined as a function of time and distance. We tested copper-plated surfaces with different degrees of roughness, as-received stainless steel surfaces, and silver-plated surfaces. Under similar environmental conditions, that is, surface temperatures of 600°F, use of helium as a coolant, and flow conditions characterized by a Reynolds number in excess of 20,000, the silver-plated and copper-plated surfaces showed a substantially greater amount of plate-out than the stainless steel surface showed.

Graphite Oxidation Experiment. - The fifth and final experiment of the present series in which we determined the rate of reaction between reactor-grade (TSF) graphite specimens and trace impurities in the helium coolant was terminated after 1080 hr of operation. The maximum graphite temperature was maintained at 1800°F, and the CO and CO₂ impurity levels were controlled at 150 and 625 ppm respectively. By visual examination

of the 12 specimens, we saw a uniform gray color and no local attack or large pitted areas. We are now making weight-loss determinations on the individual specimens.

Studies of Anisotropy Factors for Coated Particles and Pyrolytic Carbons. - A computer program was written for calculating anisotropy factors for pyrolytic-carbon coatings from x-ray data. The computer calculates the "best" M value for the data to fit a $\cos^M \phi$ equation, the σ value for a Gaussian equation, and the coefficients for a polynomial equation. Anisotropy factors are then calculated using the $\cos^M \phi$, the Gaussian, and the polynomial equations. Since the three equations do not all fit the data equally well, the three anisotropy factors are often different. Inspection of plots of the three equations reveals which equation best fits the data. For samples with low anisotropy values (5 or less), the polynomial generally fits the data best. However, samples with anisotropy values of 6 or more are best fitted with either the cosine or the Gaussian equation.

Pyrolytic-Carbon Coating Density Determinations. - Studies were made to determine to what degree of accuracy densities of pyrolytic-carbon coatings could be calculated from the routinely determined density, dimensions, and fuel content of the coated particles. We calculated coating densities for 46 lots of particles and compared them with measured values obtained by the helium pycnometer method normally used. This method requires the destruction of a 4- to 5-g sample. The average difference between the measured and calculated values was 2.74%, and the maximum difference was 6.87%. Thus we believe that it will be reasonable to estimate the coating densities for very small lots of material for which, because of prohibitive losses, density values could not otherwise be obtained.

Heat Transfer Analysis of Fueled-Graphite Irradiation Experiments. - Heat transfer calculations, based on irradiation test data, were performed for AVR-type fueled-graphite spheres irradiated in ORR poolside capsules in order to obtain (1) values for the thermal conductivity of fueled graphite during irradiation and (2) estimates of the temperature-time history of those fuel elements not containing central thermocouples. We used data from temperature-time plots for points adjacent to the surface of each fuel sphere and at the centers of two instrumented spheres, as well as the average power for each sphere obtained from flux monitor analyses and relative gamma scans. The calculated fueled-graphite thermal conductivities showed a general decrease during each irradiation subcycle, with an unexplained partial recovery between the end of one subcycle and the start of the next. We will continue this study in an attempt to provide an explanation for this unusual behavior.

REACTOR FUELS AND MATERIALS

Materials Compatibility Studies. - We have continued to determine the effect of oxygen on corrosion in the niobium-potassium system. Recently, we studied the effect of time on corrosion in the system at 815°C. After exposure for 0, 1, 25, 100, and 500 hr, niobium specimens contained 2400, 1800, 250, 130, and 96 ppm oxygen respectively. A hardness gradient

was induced in niobium in 1 hr but disappeared by 25 hr. Weight losses from the specimens were 0.8, 2.4, 2.2, and 2.1 mg/cm² during exposure times of 1, 25, 100, and 500 hr. Metallographic examination disclosed a corrosion product both in and between the grains of the specimens. The specimens contained an estimated 0.0001, 0.033, 0.036, and 0.027 vol % subsurface corrosion product respectively. The system apparently approached an effective equilibrium state at some time between 25 and 100 hr. Calculations of oxygen diffusion through niobium predicted 36 hr. The agreement suggests a corrosion process largely or entirely controlled by the presence of oxygen in the niobium.

Fuel Element Development. - We are investigating vapor deposition as a technique for forming high-temperature cladding materials. Work on the preparation of tungsten-rhenium alloys by simultaneous reduction of WF₆ and ReF₆ is continuing. We have prepared good-quality tubular deposits containing from 2 to 36% rhenium. Since ReF₆ reduces more readily than WF₆, the rhenium content in alloys deposited at 600 or 700°C was highest near the furnace inlet and fell off sharply with distance. In tubing deposited at 500°C, a 6-in. section varied from 26 to 37% in rhenium content.

The as-deposited grain structure of alloy deposits appears to depend on the rhenium content. The grain structure of a sample containing about 6% rhenium was quite columnar, resembling typical vapor-deposited tungsten. A sample containing about 22% rhenium, however, contained many areas of small grains in addition to some columnar structure.

Behavior of High-Temperature Materials Under Irradiation. - The status of the high-temperature materials experiment containing MgO, Al₂O₃, and BeO sintered compacts is summarized below:

Capsule Assembly	Approx Maximum Fast-Neutron Dose (nvt)	Temperature (°C)	Specimen Size (in.)	Status
	(× 10 ²¹)			
15	2.4	150	0.5	Hot-cell disassembly completed
16	2.4	150	0.25	Undergoing hot-cell disassembly
17	1.5	150	0.5	Hot-cell disassembly completed
18	1.5	150	0.25	Undergoing hot-cell disassembly
19	10.0	800, 1100	0.5	Undergoing irradiation
20	10.0	800, 1100	0.25	Undergoing irradiation
21	3.9	800, 1100	0.5	Hot-cell disassembly completed
22	3.9	800, 1100	0.25	Undergoing hot-cell disassembly

Gross-damage observations and dimensional measurements of the specimens of capsule assemblies 15, 17, and 21 are complete, and the data are being evaluated.

Fabrication was completed on capsule assemblies for the first irradiations of refractory carbides. These units are for uninstrumented, water-cooled experiments and are now ready for sample loading. The auxiliary hardware for the high-temperature instrumented irradiation is being fabricated. A computer program was developed for determining the dimensions of capsules that have been designed to irradiate carbide samples at temperatures up to 1400°C.

FUNDAMENTAL HEAT TRANSFER AND FLUID DYNAMICS

Vortex-Flow Hydromagnetic Stability Theory. - An exact solution describing the hydromagnetic stability of nondissipative, conducting Couette flow between two coaxial cylinders under the action of an externally applied axial magnetic field was obtained. We deduced algebraic expressions for determination of the criterion for hydromagnetic stabilization of Couette flow profiles of the form $(L/r) + Mr$, where L and M are constants and r is the radial coordinate. The parameters that determine the stability criterion were found to be the peripheral Alfvén modulus, A , the radius ratio of the cylindrical walls, κ , and a dimensionless parameter, λ , characterizing the shape of the velocity profile. We obtained numerical results for different values of κ and λ . For small ratios and small λ , the criterion converges toward the criterion for pure vortex flow.

Boundary-Layer Transient Phenomenon. - Techniques are being investigated for fabricating reliable, long-lived, hot-film surface probes for the measurement of the local, instantaneous heat-transfer rate and the coefficient of heat transfer. We are currently evaluating vacuum evaporation onto a cast epoxy rod containing two electrodes for ease of forming the film, for endurance, for dimensional and electrical stability, etc. Gold appears to be a satisfactory material for this purpose. A new test section, consisting of a 2-in.-diam, polished, chrome-plated brass tube with four hot-film surface probes and a hot-film anemometer, was fabricated.

Recently we measured the instantaneous, local, water-film heat-transfer coefficient inside a 2-in.-diam pipe containing a single hot-film probe that formed one leg of a constant-temperature hot-film anemometer bridge. Data for a Reynolds modulus of 17,000 were analyzed manually to ascertain the spectral distribution of the observed fluctuations in the local film coefficient. Maximum fluctuations of ± 9 to $\pm 12\%$ about the mean were found to occur in the low-frequency range from 1 to 2 cps, decreasing to 1 to 2% in the high-frequency range above 20 cps. Average values of the fluctuations range from $\pm 9\%$ at the low end of the spectrum to $\pm 0.6\%$ at the high end. We believe that the low-frequency fluctuations are of greatest significance from the standpoint of thermal fatigue damage to metals.

Boiling Alkali-Metal Heat-Transfer Studies. - An investigation was undertaken of the superheat required to initiate boiling and of the relation between superheat and boiler-wall temperature fluctuations with

boiling sodium. We are carrying out the experimental phase of this work in the 20-in. natural-convection loop described previously. Three boiler test sections were used in these studies: (1) an as-received 1/2-in. sched 40, type 347 stainless steel pipe; (2) an 8-in. length of the 1/2-in. pipe containing eight 0.006-in.-diam holes arranged in two diametrically opposite axial rows of four holes at 2-in. separation (the rows are offset by 1 in. in the axial direction with respect to each other); and (3) an 8-in. length of the 1/2-in. pipe with a sintered stainless steel surface. In these studies we intend to evaluate the effects of surface treatment and heat flux on the superheat required to initiate boiling at various saturation temperatures, the stability of the boiling process, and the amplitude and frequency of the boiler-wall temperature fluctuations. In addition, we will compare the data obtained with boiling sodium, and correlate it, when possible, with data previously obtained with boiling potassium.

A preliminary evaluation of data obtained with sodium and with potassium indicated that both of the treated surfaces had a stabilizing effect on the boiling process and tended to reduce the amount of superheat required to initiate and maintain boiling. A summary of boiling sodium and potassium data we obtained with the 20-in. natural-circulation loop follows:

Surface	Range of Saturation Temperature (°F)	Range of Superheat (°F)	Range of Heat Flux (Btu hr ⁻¹ ft ⁻²)	Maximum Wall Temperature Fluctuation (°F)
Potassium				
Smooth	1099-1766	456-177	21,980-36,753	>300
Sintered	968-1554	239-22	20,000-33,683	85
0.006-in.-diam holes	875-1548	397-7	21,140	21
Sodium ^a				
Sintered	927-1624	630-48	9,570-20,784	57
0.006-in.-diam holes	1342-1684	103-28	13,124-22,975	34

^aNo data were obtained for the smooth surface.

POWER REACTOR FUEL PROCESSING

Chemical Analysis of Advanced Reactor Fuels: Determination of the Nitric Acid Oxidation Products of Carbide Fuels. - The pyrolysis of several polycarboxyl aromatic acids is being studied in an attempt to find an analytical method for evaluating the concentrations of the various

solid acids formed in the hydrolysis of the uranium and thorium carbides on dissolution in HNO_3 solutions. The hydrolyzed samples are introduced into a tube furnace at approximately 900°C . A constant stream of helium over the sample carries the pyrolysis products into a gas chromatographic system. In all cases observed to date, the principal products have been carbon monoxide and carbon dioxide, with lesser amounts of ethylene, acetylene, benzene, and toluene. The presence of some 20 other high-boiling constituents is also indicated by the chromatograms.

Cyclic Dissolution of Irradiated Sol-Gel $\text{ThO}_2\text{-UO}_2$. - Stainless-steel-clad vibratorily compacted $\text{ThO}_2\text{-UO}_2$ capsules prepared by the sol-gel process were irradiated in the NRX reactor to burnups of 13,000 to 17,000 Mwd per metric ton of thorium plus uranium and decayed about 2 years. The capsules were then declad by the Sulfex process, and the core oxide was dissolved over eight cycles; the "heel" procedure was used. Losses of thorium plus uranium to the 6 M H_2SO_4 decladding solution averaged 0.50% for the eight sectioned rods. After three cycles, batches of exposed core oxide were dissolved to produce a 1 M Th concentration in a 13 M $\text{HNO}_3\text{-0.04 M KF-0.04 M Al(NO}_3)_3$ reagent. A 5-hr dissolution period was used. The constant heel after the fifth cycle represented about 5% of the total material charged to the system and consisted of fuel oxide (2.5% of the 532 g charged), undissolved stainless steel cladding, and $\text{SiO}_2\text{-Al}_2\text{O}_3$ from the Fiberfrax wadding in the fuel rods.

Batch Leaching of Irradiated $\text{ThO}_2\text{-UO}_2$ Pellets. - Helium-bonded, stainless-steel-clad $\text{ThO}_2\text{-UO}_2$ pellets of the Consolidated Edison type were irradiated in the ETR to 52,000 Mwd/metric ton as experiment ORNL 43-44 and in the MTR to 102,000 Mwd/metric ton as experiment ORNL 43-40. The pellets, which had a density 95% of theoretical, were then decayed 2 years.

Sections approximately 1 in. long of the specimens remaining from metallographic examination were leached in boiling Thorex reagent (13 M $\text{HNO}_3\text{-0.04 M KF-0.04 M Al}$) to 0.5 M and 1 M terminal thorium concentrations in about 9 and 24 hr respectively. Light-gray insoluble residues, amounting to 0.25 to 0.75% of the total oxide charged to the systems, were analyzed by emission spectroscopy; they contained principally silica and alumina, along with moderate amounts of fission product molybdenum and corrosion product iron, chromium, and nickel from the stainless steel and traces of other elements. The $\text{ThO}_2\text{-UO}_2$ content of the residues was from 0.003 to 0.02% of the total oxide charged.

Pyrohydrolysis of HTGR and Coated-Particle $\text{ThC}_2\text{-UC}_2$ Fuels. - A series of runs with HTGR fuel and coated-particle $\text{ThC}_2\text{-UC}_2$ samples were conducted in the laboratory-scale pyrohydrolysis equipment. Five-gram (nominally) samples of HTGR compact 4 (11.6% Th, 5.6% U, and 82.8% total carbon) were exposed to flowing steam at 2.45 liters/min, temperatures from 600 to nearly 800°C , and atmospheric pressure, with no evidence of reaction. At 800°C , slight reaction was indicated by the production of a noncondensable off-gas flow of 17 ml/min. This off-gas flow rate was about a tenth of that obtained by the pyrohydrolysis of uranium or plutonium monocarbide under comparable conditions. In this test the temperature could not be further increased because of the limited capacity of the resistance furnace. The run was not completed, but calculations indicate that about 20 hr would have been required to complete the pyrohydrolysis.

Pyrohydrolysis was also attempted with coated particles made by the Minnesota Mining and Manufacturing Company. The particles were 150 to 250 μ in diameter and consisted of 82% $\text{ThC}_2\text{-UC}_2$ with an 80- μ coating of pyrolytic carbon. They were totally nonreactive toward steam at 800°C. These results suggest the possibility of recovering the coated particles intact from HTGR fuel by selective pyrohydrolysis of the graphite matrix with steam at 300°C or higher. Small-scale recovery of coated-particle fuel is currently done by General Atomic by crushing and wet-chemical or electrochemical oxidation.

Further investigation of the pyrohydrolysis of these fuel types will be conducted at higher temperatures (up to 1000°C), with catalysts to possibly increase the reaction rate.

Reduction of Plutonium with Hydrogen. - Methods that do not contribute impurities to the plutonium or solids to the aqueous waste streams are being studied for the selective stripping of plutonium from organic solutions. In laboratory experiments, plutonium was reduced from Pu(IV) to Pu(III) by the use of 4% H_2 in argon and a platinum catalyst. An organic solution of uranium and plutonium (95 g of uranium per liter, 1 g of plutonium per liter, 0.1 M in H^+ , in 30% TBP) was stripped in a column with an aqueous solution 0.5 M in H^+ . The Ar-4% H_2 was passed upward through the column, which was packed with platinized alumina. After about a 10-min holdup in the column, about 99.8% of the plutonium had transferred to the aqueous phase.

THORIUM UTILIZATION PROGRAM

Ultrasonic Dispersion of Carbon Black in Sols. - Studies of the dispersion of carbon blacks in thoria-urania sols and in toluene by use of an ultrasonic dispersion device and surfactants were continued. A uniform dispersion of carbon in sols is of interest because it is a necessary property for carbide formation and for one approach to the development of controlled porosity in oxides.

Sols 2 M in thoria, 0 or 0.06 M in urania, and 0 or 8.4 M in carbon were dispersed in hexane, gelled in diethylenetriamine, washed with acetone, and calcined to give oxide microspheres. When the 2 M thoria sol was used, the spheres had densities of 8.92, 8.87, and 8.84 g/cm^3 after calcination at 850°C. When the sols that were 8.4 M in carbon were used, the thoria or thoria-urania spheres were badly cracked after calcination in air at 850°C. One sample of thoria spheres prepared from a 2 M thoria-8.4 M carbon sol had a density of 7.7 g/cm^3 after air calcination at 850°C.

Thorium-Uranium Fuel Cycle Development Facility. - Building design progressed to approximately 40% completion. Minor revisions in design are being made in order to improve operability or to reduce costs and ease possible procurement problems. The purchase order for the in-cell crane and manipulator system was placed for slightly less than \$350,000.

Testing of the vertical tube furnace began, as did preliminary design of the alternate furnace. The sol-gel flowsheet is being reviewed and revised.

Work continued on the various equipment items required for oxide fuel rod fabrication along the lines previously established, except in two cases. In the first, the design requirement for a helium-leak-test device for the fuel rods was changed from testing a number of rods simultaneously to testing each rod singly. In the second, an alpha monitor is being considered as a substitute for a mechanical smearing device for determining surface contamination.

Chemistry of the Separation of Protactinium from Thorium in Molten Chloride Salts. - Experiments employing neutron irradiation of mixtures of AlCl_3 and ThCl_4 to explore the possibility of removing bred ^{233}Pa by volatilization were continued.

Volatilization of half the AlCl_3 from a mixture containing 2 mole % ThCl_4 resulted in the transfer of 7% of the protactinium activity. Distillation experiments in which quartz wool was included in the receiver or in the original salt region showed that the quartz wool in the receiver held the protactinium that had been distilled from irradiated AlCl_3 containing 0.5 mole % ThCl_4 . Quartz wool in the salt region from which distillation occurred, however, did not entirely prevent the distillation of protactinium.

Preparation of Sol-Gel ThO_2 Having Controlled Porosity. - Sol-gel ThO_2 fragments (-6 +16 U.S. mesh size) were made slightly more porous than normal sol-gel material by decreasing the firing temperature from 1150 to 900°C. The fragments dissolved more than 10 times as fast as the normal material in 13 M HNO_3 -0.04 M HF -0.04 M $\text{Al}(\text{NO}_3)_3$. Much of the surface-connected porosity consisted of pores less than 200 A in diameter, too small to admit mercury at 8000 psi, but large enough to admit water.

The porosity of sol-gel thoria was also increased in direct proportion to the amount of carbon added at the sol stage, when the sol was dried and fired in air. The residue of carbon in the product was less than 0.01%.

Development of Equipment for Microsphere Preparation and Coating. - Formation of fuel microspheres by introducing aqueous sols of fuel material into a column of immiscible liquid drying agents, such as long-chain alcohols, shows promise as a near-universal method for making gel spheres that can be calcined to ceramic fuel.

Various column configurations are being studied. A tapered column with a tangential inlet of the fluidizing solvent and a 1-1/2-in. minimum diameter was used throughout July. Continuous operation, in which dried gel microspheres drop out of the bottom while wet sol drops are being fed into the top, was consistently possible.

Fabrication and installation of a distillation system to remove water from the solvent and of a tapered column of improved configuration with a 2-in. minimum diameter are partially complete. When this apparatus is completely installed and the sol feed pumps for additional dispersion nozzles are received, the system should have a continuous capacity of over 3 and perhaps over 10 cm^3 of sol per minute.

In an effort to measure the height of fluidized beds in particle coat-ers, a system consisting of a light source and collimator, a photo-electric cell, and a recorder was built. The principle of this device is to measure the light attenuation of the fluidized bed in a glass column. In an actual operating bed, a gamma or an x-ray beam will replace the light.

Development of Fuel-Rod-Homogeneity Scanner. - Gamma scanning is being used to determine fuel homogeneity in fuel rods. The effects of fuel radioactivity and background radiation are being studied.

An experiment was completed for determining the allowable background for the crystal photomultiplier radiation detector. It was shown that a background of 1 mr/hr (produced with ^{137}Cs) was equivalent to an approximately 2% change in the fuel of a 1/2-in.-diam fuel rod. This radiation level can be tolerated and easily biased from the system since the measurements are all relative to the standards and are not absolute. A background of 0.25 mr/hr or less produces no apparent deflection on the recorder.

Calculations were also made in order to determine the self-emitted radiation levels from the rod through 1/8-in.-diam collimation through various thicknesses of lead on the particular rod being scanned. About 10 in. of lead will be needed for 1-kg rods with fission products in order to reduce this level of radiation to an insignificant amount. Five-kilogram rods with fission products are not being considered for these criteria.

Development of Thorium-Uranium Fuel Cycle Facility Equipment. - The vertical tube furnace must be proved operable by November to meet present schedules of the Thorium-Uranium Fuel Cycle Development Facility. If the furnace becomes inoperable at any time, a second furnace must be selected and built quickly. The testing of the vertical tube furnace consists in the following: testing the product-removal mechanism by using a 3-in. aluminum pipe to represent the furnace and sized gravel to represent the sol-gel oxides; testing the complete system, including the controls, at temperature, both empty and with used sol-gel product; and continuous, full-scale operation with gel feed.

The furnace-product-removal mechanism was sent to our shops to correct poor-quality work by the original fabricator. The instrument panel was received, and power-supply equipment was ordered to permit parallel operation of the Globar heating elements. Failure of one or two elements might be tolerable for parallel operation; the whole group would be lost if one element in a series arrangement fails.

Vibratory Compaction. - In a continuing study of vibratory compaction, the relationship between bulk density and length of floating guide incorporated into a NAVCO BH 1-5/8-in. pneumatic vibrator was studied. In general, the bulk density obtainable appears to be independent of the length of the guide at air pressures below 50 psi; above 50 psi, some anomalous length effects have appeared. These anomalous effects are now being examined in greater detail. Three guides, 6-1/2, 4-1/2, and 2-1/2 in. long, were studied, and all yielded bulk densities that are in general agreement with those obtained with the 8-1/2-in. guide.

Completion of the Kilorod Program. - The last of the ThO_2 -3% $^{233}\text{UO}_2$ pellets for use at Brookhaven National Laboratory (BNL) in the ThO_2 - $^{233}\text{UO}_2$ criticality experiments have been fabricated. They will be sent to BNL when the shipping cask is received.

Dissolution of the analytical samples and cleanout of the Kilorod Facility have continued. So far, about 48 kg of the ThO_2 - UO_2 has been dissolved. About 28 kg remains to be dissolved.

Coated-Particle Development Laboratory. - Modifications to room 241, Building 4508, to adapt it to microsphere preparation are being carried out by the H. K. Ferguson Company. An order was placed for the graphite resistance furnace to be used in pyrolytic-coating scale-up studies, fabrication of the graphite coater internals was completed, and the stainless steel parts are being built. Bids for the glove box were sent out, and purchase will be made within three weeks. Requests have been sent out for estimates for fabrication of the enclosures.

Irradiation of Thorium Oxide Fuels. - Irradiation tests will be made on ThO_2 -3% $^{233}\text{UO}_2$ rods that are essentially the same as the 19-in. rods prepared in the Kilorod Program. So far, attempts to fabricate these test rods have been unsuccessful because of weld failures during autoclaving tests. A second group of prototype fuel rods has now been remotely fabricated utilizing BNL archive fuel but with greater control on the size distribution and increased sampling for detailed characterization of the fuel. The current program calls for irradiation of six of these rods in the Materials Testing Reactor - three with production oxide and three with refired oxide. The rods are designed to operate at an average heat flux of $628,000 \text{ Btu hr}^{-1} \text{ ft}^{-2}$, with a surface temperature of 205°F , to a maximum burnup of approximately 100,000 Mwd per metric ton of uranium and thorium. The rods will be shipped to the reactor site in Idaho about September 1.

Gas Evolution from Sol-Gel ThO_2 -3% UO_2 . - Gas evolution invoked by heating sol-gel-prepared ThO_2 -3% UO_2 to high temperatures in vacuum is being reinvestigated. The early work, carried out over two years ago, has been reviewed, and a detailed study of the factors affecting the evolution of gases from thorium-uranium oxide particles obtained from the sol-gel process has begun. Apparatus was constructed for the measurement and collection of the gases liberated under controlled temperature conditions, and calibration of the equipment is complete. The results to date indicate that small gas samples can be measured accurately.

From results recently obtained, it appears that the procedure for outgassing adopted in the early work - heating in vacuum at 1200°C - may not be adequate to release all the gas trapped in the coarse fraction of particles. It was found that grinding the coarse fraction in an argon atmosphere after it had been outgassed for as long as 30 min at 1200°C resulted in evolution of additional gas in amounts up to ten times the amount originally evolved from the coarse fraction.

In further preliminary outgassing experiments carried out with ThO_2 -3% UO_2 obtained as -6 +20 mesh particles from the standard sol-gel process, the total gas evolved at 1000°C was about $0.015 \text{ std cm}^3/\text{g}$. The oxide was handled in air. The liberated gas consisted of CO_2 , O_2 , N_2 , and small amounts of CO and H_2O . Grinding, in this case in air rather than argon, resulted in further evolution of gas, approximately half of which was shown to be due to adsorption from the air during grinding. After grinding of the original oxide to -30 mesh in air, the evolved gases totaled $0.13 \text{ std cm}^3/\text{g}$. The approximately tenfold increase in gas evolved after grinding agrees well with the above experiment in which grinding was carried out in argon.

Extension of Sol-Gel Process to Newer Fuel Types. - Various mixtures of thoria with other materials are of interest for newer fuel concepts. Zirconia sol preparation and a cermet of thoria and tungsten were studied this month.

Preparation of zirconia sols from zirconyl nitrate by denitration above 100°C with steam dehydrates the oxide irreversibly, rendering it nondispersible. However, a stable zirconia sol was produced by reducing the nitrate with formic acid to an $\text{NO}_3^-/\text{ZrO}_2$ mole ratio of approximately 1. The sol was formed to gel microspheres in 2-ethylhexanol and then fired to oxide spheres having a particle density of 4.9 g/cm³.

When tungsten in the form of particles less than 1 μ in diameter was added to ThO₂ sols, a precipitate containing up to 50 wt % ThO₂ was formed. A compact was prepared from this precipitate in which the ThO₂ content was 4.22 wt %. The compact was fired at 1800°C under 1200 psi for about 1/2 hr. The density of the product was 80% of theoretical, and, from metallographic sections, the metal phase was continuous.

Permeability of Vibratorily Compacted Fuels. - The experimental apparatus to study the interaction of heat-up rate, degree of waterlogging, fuel permeability, and pressure rise in vibratorily packed fuel rods was completed. Exploratory runs were made in order to determine operating conditions. The initial test assembly simulates a vibratorily packed fuel element 14.3 cm long with a 0.71-cm² cross section and with a leak in one end. With a test fuel body compacted from sol-gel thoria having a particle-size distribution similar to that used in the Kilorod fuel rods, the water and gas permeabilities were determined to be 0.97×10^{-4} and 7.4×10^{-4} respectively. The ratio of these values, 7.6, fits the pattern of previous results.

MOLTEN-SALT REACTOR PROGRAM

Molten-Salt Reactor Experiment. - The heat exchanger was installed in the reactor cell, together with the remaining removable heater-insulation units. This completes the installation of major components, leaving only final electrical and service connections to be made.

The change room and the south containment wall were completed. Work continued on the tanks for the vapor-condensing system and the installation of the fuel-reprocessing system. Progress continued to be made on electrical and instrumentation wiring installation. The remaining heater-insulation units for the drain tank cell were delivered.

On August 1, the critical-path schedule showed the project to be 95.8% complete.

MSRE Operations. - Training continued for the MSRE operators, with emphasis on an understanding of the process flowsheets and the control circuitry.

A large number of visitors, from industry and from the Laboratory, toured the reactor area in connection with the MSRE semiannual information meeting. Exhibits had been set up explaining the development and construction of the MSRE, and the operators served as guides.

Preparation for the use of the on-line digital computer continued on schedule. Plans for use are complete, and over half of the program

has been written. The programming is a joint effort of the computer manufacturer and ORNL, with the manufacturer handling the input scanning and data acquisition and ORNL handling the computations and the printed output.

Development of Components and Systems. - Shakedown runs for each of the three reactor control rods were completed. Each rod was operated through 5000 cycles at 1200°F and scrambled a minimum of 50 times each. The rods are ready for use in the reactor.

Two uranium additions were made to the engineering test loop. They raised the uranium concentration first to about 0.4 mole % and then to about 0.74 mole %. The concentration by chemical analysis agreed with the predicted value within 1% at the higher concentration; however, the agreement was not so good at the lower concentration, possibly a result of a difference in the method of loading into the loop. Visual examination of a bar of graphite removed from the loop indicated no change after 7000 hr of operation with fuel salt.

Testing of the reassembled heat exchanger was completed, and no audible vibrations were noticed that could be attributed to tube vibration. The pressure drop through the shell side was measured and found to be slightly higher than was measured with the stainless steel test shell.

Preparations are being made for testing of the maintenance system in the reactor cell. Monitoring the construction and installation of reactor equipment is continuing. With the installation of the reactor vessel and pump bowl has come the adjustment and testing of the remote maintenance lift fixtures for these components. The original design worked well and needed no revision. A mockup was made which included revisions in the design for the graphite sampler, and tools and techniques for handling the samples were tested and found satisfactory.

MSRE Pump Program. - The coolant pump rotary assembly and its drive motor were delivered to the MSRE. The assembly of two spare rotary elements for the MSRE salt pumps was started, and one of them is being installed into the cold shakedown test stand. Fabrication of the components for the rotary assembly of the MK-II fuel pump was completed. Attempts to calibrate a radiation densitometer to measure the concentration of undissolved gas in circulating water in the water mockup of the MK-II fuel pump tank revealed a change in calibration with time. The adequacy of the stability and response of the complete densitometer device to measure concentrations of undissolved gas is being studied.

Instrument Development. - Four resistance thermometers, rated for short-term operation at 1400°C, were operated at 1350°F, to determine the feasibility of using resistance thermometers to obtain precision temperature measurements under conditions of long-term operation at MSRE temperatures. Two of the four thermometers became erratic shortly after the start of the tests. One of the remaining two thermometers, supplied by a different manufacturer, also became erratic after 1250 hr of operation. The performance of the fourth thermometer remained stable after 1850 hr of operation. These tests have now been terminated, and the data are being analyzed to determine the magnitude and rate of drift. An attempt will be made to determine the cause of the three thermometer failures.

The program of assistance in the design, fabrication, and testing of an ultrasonic molten-salt level probe is continuing. Modifications

of an existing molten-salt level test facility have been completed. A probe assembly design submitted by the contractor (Aeroprojects, Inc.) was reviewed and revised as required to satisfy reactor systems design and containment criteria. A probe assembly was fabricated in ORNL shops and returned to the contractor for testing. Field testing of the level probe system will commence when the tests of the probe assembly by the contractor are completed.

A motion-multiplying device was designed and developed for use in obtaining a 1-in. stroke, required by some of the valves in the MSRE, from all-metal pneumatic bellows-sealed valve actuators. These bellows actuators, which were tested and proved in HRT operation, were available as surplus at ORNL. The motion multiplier is basically a rolling-wheel device in which the actuator motion is applied to the axis of the wheel. The motion is transmitted to the valve stem by an Elgiloy tape. Since the device uses a commercially available flexure pivot for the wheel axis and does not require lubrication, it is acceptable for use in inaccessible locations and in high-radiation environments such as are found inside reactor containment vessels.

Testing of the prototype ball-float type molten-salt level indicators has been terminated. The two systems installed on the prototype test facility operated satisfactorily for 29 months. Calibration made at the end of the test indicated a change in sensitivity for both systems of ± 0.2 in. for a 5-in. range.

After the final calibrations were completed, the system in which the differential transformer core was suspended below the graphite float was removed from the test loop and inspected. A visual check of the graphite float showed no deterioration of the graphite. There was no visible indication that molten salt had penetrated the graphite, and no granulation of the surface had taken place. Machine marks made when the surface of the float was being finished were still visible. The INOR-8 core tube, which had been immersed in the salt for this entire period, was still clean. There was some indication that the nickel wire used in winding the differential transformer may have become brittle, since one lead wire broke at the point at which it entered the transformer when the transformer was disassembled. Twisting the end of the broken wire caused it to break again. Further tests will be performed to determine the extent of embrittlement after the present electrical characteristics of the transformer have been determined.

The pump bowl level indicator installed on the MSRE prototype pump test loop has operated satisfactorily since installation. This system is sensitive and repeats very well. Some difficulty has been encountered in obtaining an accurate field calibration of the transmitter. A laboratory setup was made and used to determine the procedure necessary to eliminate the calibration difficulty.

Installation of a ball-float level indicator on the MSRE coolant system pump has been completed.

NUCLEAR SAFETY

Release of Fission Products During Melting of Fuels Under Transient Reactor Conditions. - A series of experiments is being performed in the

TREAT facility to study the release of fission products from fuel melted under transient reactor conditions. Radiochemical analyses of the third and fourth experiments have been completed. The fuel in these experiments had been given a preliminary irradiation in order to permit study of the behavior of long-lived fission products rather than that of their short-lived precursors. The fuel in each experiment was melted in an air-steam atmosphere. Details of the transients and of the results of physical examinations of the specimens after the transients were given in a previous report (ORNL-3663).

Given below is a summary of the distribution of aged fission products and of UO₂ in experiments 3 and 4.

Summary of Distribution of Aged Fission Products and UO₂ in TREAT Experiments (% of inventory)

Release Zone	¹³¹ I	¹²⁹ Te	¹³⁷ Cs	¹⁰⁶ Ru	⁸⁹ Sr	¹⁴⁰ Ba	⁹⁵ Zr	¹⁴⁴ Ce	UO ₂
Experiment 3									
Total release from UO ₂ fuel	45	32	38	8	2	3	4	3	3
Release from high-temperature zone	7.0	0.83	1.2	1.5	0	0.7	1.0	0.92	0.8
Transported release ^a	1.2	0.10	0.22	0.0007	0	0.7	0.0006	0.0003	0.000
Experiment 4									
Total release from UO ₂ fuel	41	28	31	1.2	1.6	3	0.6	0.2	0.66
Release from high-temperature zone	8.2	0.70	1.6	0.031	0.56	1.2	0.003	0.002	0.00
Transported release ^a	1.4	0.25	1.2	0.026	0.56	1.2	0.002	0.002	0.00

^aTransported release is material transported from the fuel autoclave into the aerosol-transport zone and gas-collection autoclave.

In these experiments the transient release of aged fission products from UO₂ was shown to be less than the release of fission products formed during the transient. This is apparently related to the fact that the recently born fission products occur in elements that are generally more volatile than their daughters. A comparison of the transient release values for aged fission products with data on the release of aged fission products during slow melting obtained by other ORNL experimenters showed that the pattern of release was similar and that the percent release was less for transient heating in all cases. Release values for the low-volatility fission products strontium, barium, zirconium, and cerium were approximately equal to the percentages of uranium volatilized in both types of experiments. Large fractions of the volatile fission products were released from the fuel, but most of these materials remained in the high-temperature zone. In these transient release experiments, approximately one-third of the volatile fission products iodine, tellurium, and cesium was released from the fuel, but only 1% was released from the fuel autoclave.

Properties of Fission Product Aerosols Produced by Overheated Reactor Fuels. - The effect of pressurization of the atmosphere in the Confinement Mockup Facility (CMF) has been studied with air and a steam-air mixture. Comparison of the results obtained indicates the effect of steam on the deposition and desorption processes. Another objective of the studies was to provide a realistic determination of the maximum amount of iodine available for leakage from the containment during depressurization. Earlier data (ORNL-3363) based on a gas displacement method gave values between 30 and 60% for the total amount of iodine which could be desorbed from the confinement tank after 4 hr of aging.

The experimental conditions used included essentially clean atmospheres, and the transport processes observed were not influenced by such factors as organic materials or vaporized material from overheated fuels.

The principal results are indicated in the table below.

Behavior of Iodine in the Containment Mockup Facility Filled with Filtered Air and with Steam-Air Mixture Under Pressure

Iodine Distribution	Percentage of Inventory	
	Filtered Air at 15 psig	Steam (10 psig)-Air (15 psig)
Amount in the containment tank:		
Retained on tank walls	79.5	19.3
Collected in steam condensate		52.9
Total retention	79.5	72.2
Iodine removed from containment tank by:		
Air pressure release (to 0 psig)	2.9 ^a	13.0 ^a
Argon displacement ^b (2-3/4 tank volumes)	7.4	13.3
Air sweep (2.5 tank volumes)	2.9	0.5
Total removed	13.2	26.8
Iodine collected by test samples (40 cm ²):		
Stainless steel	0.1	0.05
Mild steel	3.6	0.4
Alkyd painted steel	2.4	0.3
Total collected on test samples	6.1	0.8
Amount penetrating screens and charcoal papers	0.1	16
Loss through 1.5 in. of charcoal	0.001	0.4

^aThis amount represents the maximum possible leakage from a containment system.

^bThe time interval between the argon cycle and the air cycle was 8 hr in the "air" run and only 1 hr in the "steam and air" run.

They show that the change from air to a steam-air atmosphere had no significant influence on the amount of iodine retained in the tank (70 to 80%), although the presence of moisture reduced the fraction of iodine which remained on the tank wall from about 80 to 20%. The difference can be ascribed chiefly to the amount of iodine in the steam condensate (53%).

The overall effect of the steam was to increase the amount of iodine available for removal from the containment tank during depressurization from 2.9% in the dry system to 13% in the wet system. A secondary effect of the steam was to prevent the adsorption of iodine by the silver-plated screens and charcoal papers, causing it to collect in the charcoal beds. In the dry system the amount of iodine found in the charcoal beds was 0.1% of the total, and in the wet system it was 16.3%. The amount that penetrated through 1.5 in. of charcoal increased from 0.001 to 0.4% in the presence of steam.

Since we lack any indication of a reason for the iodine to be in a more penetrating form in the presence of steam, it is presently assumed that the distribution of iodine observed in this experiment was due to competition between the iodine and water molecules for the surface of the charcoal. Experiments with heated charcoal and diffusion tubes are planned, to test the validity of this assumption.

A comparison of the plate-out process (on 40 cm² of test samples) in air with that in steam also showed a wide variation in the total amount of iodine on all test samples (from 6.1% in air to 0.8% in steam). The ratio of the percent of iodine adsorbed in air to that adsorbed in steam for the three types of surfaces was 2 for stainless steel, 8 for painted steel, and 9 for mild steel. The data suggest that the steam condensate decreases the available surface for adsorption and that it also washes off some of the adsorbed material, as shown by the fact that 53% of the total iodine was found in the condensate (245 cm³).

Behavior of Fission Products on In-Pile Destruction of Reactor Fuels.

- Two experiments were recently performed on the behavior of fission products released during in-pile melting of fuel. Miniature stainless-steel-clad UO₂ fuel elements were melted for a 5-min period in each experiment. In the first, the sweep gas was dry air flowing at 50 std cc/min. In the second, water was supplied to the sweep gas so that a steam environment was present during the time the fuel was molten. The steam-air flow rate in the second experiment was 400 cc/min.

Physical examination of these experiments during disassembly in the hot cell showed that they were very similar. The fuel had melted in each case, and no unoxidized stainless steel cladding could be seen. The filters in the second experiment were more heavily coated than those in the first experiment; this is attributed to the differences in sweep-gas flow rates. Radiochemical analyses of the experiments are 90 and 75% completed respectively.

Characterization, Control, and Simulation of Accident-Released Fission Products. - Composite diffusion tubes, developed to characterize various vapor forms of radioiodine, are usually arranged with successive inner surfaces of silver, rubber, and activated carbon, all at about 25°C. An experiment was performed in which this arrangement was varied, in order to investigate certain previously observed phenomena. Iodine, prepared

by the dichromate method, was used with fairly dry filtered air. The effect of heating on diffusion tube performance was investigated at the same time, as a preliminary to determining the feasibility of using diffusion tubes for analyzing iodine in air containing steam. Adsorption of moisture and its consequent interference would be reduced by increasing the temperature of the diffusion tube surfaces.

This experiment yielded a variety of information, the more important of which will be presented here. The occurrence of at least two distinct iodine species other than I_2 was indicated; one of the species appears to be relatively unstable, with HI or I_2 as a probable decomposition product. The depositions obtained on the rubber sections of the diffusion tubes were not simple diffusion-controlled depositions but were considerably more complex. In this particular study, iodine carried by particulates was contra-indicated. A diffusion tube at $100^\circ C$ yields an altered but interpretable distribution, and the usefulness of this method for analyzing the various species of radioiodine present in a moist atmosphere is to be investigated further.

Nuclear Safety Information Center. - In order to expand the services it can offer, the Nuclear Safety Information Center will soon be able to use a computer for the preparation of routine bulletins of the Center's accessions and for making retrospective searches of the Center's files. Programming for the IBM 7090-IBM 1401 facilities at the ORGDP are currently under way.

During July and August the Center received and answered 15 specific requests for information. In the same period eight persons visited the Center to consult with its staff specialists. The Center's latest state-of-the-art study, Current Practices in the Release and Monitoring of I^{131} at NRTS, Hanford, Savannah River, and ORNL, has been completed and has received wide distribution in the nuclear community.

Technical revision of the first draft of the Reactor Containment Handbook is now complete as is the index for it. The manuscript is now being edited and will be published as a final draft in November - its release is subject only to AEC review.

Nuclear Safety Pilot Plant. - The behavior of iodine released into the Model Containment Vessel (MCV) has been studied using an air atmosphere. Two experiments have been completed where 100 mg of ^{127}I and 10 mc of ^{131}I were vaporized in the plasma torch furnace. The first specimen was stainless-steel-clad EGCR-type UO_2 pellets with the iodine packed in the central void space of the pellets. In the second, the iodine was contained in a Pyrex ampul.

The UO_2 test was made without the use of the fan installed in the MCV. The results indicate nonuniform mixing in the vessel, with the concentrations in the top of the vessel, near the gas inlet, initially being orders of magnitude greater. The iodine distribution was similar to the UO_2 distribution during the first several hours, but nonparticulate iodine was predominant after this initial period. Data from the tape air sampler, which included roughing paper, a Millipore filter, and charcoal paper, showed that the iodine decreased by less than two orders of magnitude from the peak value during the 24-hr experiment; however, the percentage of the iodine on the charcoal paper increased from 45 to 97% during this time.

The experiment using only iodine gave results similar to those of the UO₂ capsule run, although the fan was run for the first 15 min of the experiment in order to give thorough mixing in the containment vessel. Deposition coupons at three elevations in the vessel gave almost identical values for deposited iodine, as did the carousel fallout sampler and the larger fallout cups located at the bottom of the MCV. The tape air samplers showed a decrease in the iodine concentration of one order of magnitude from the peak value during the run.

The May pack sampler was installed for this latter run. This device is also remotely operated and has 12 separate samplers, each consisting of a combination of filter media: Millipore, silver screens, charcoal paper, and charcoal beds. The results indicate that a very high fraction (85.95%) of the iodine was removed by the silver screens during the first 30 min of the run, with the bulk of the remainder divided equally between stainless steel support screens, Kel-F containers, charcoal paper, and charcoal beds. Very little iodine (less than 0.2%) was observed on the Millipore paper. During the remainder of the experiment the silver screens removed the largest portion of the iodine again, but an increasing fraction was noted in the charcoal beds (5.38%) and charcoal paper (0.5-4.0%).

RADIOACTIVE WASTE DISPOSAL

Clinch River Study. - Dye tracer tests were conducted in the first week of April 1964 to study the effects of power releases on the diffusion of radioactive releases from White Oak Lake into the river during winter conditions. The tidal estuary model, first used to predict the effects of dye diffusion in the summer condition tests of 1963, has been further refined. In its application, comparison between observed and theoretical concentrations of dye, at downstream points in the Clinch River for winter conditions, has been very good.

A computer program has been developed for comparison of variations in gross gamma radioactivity with depth in Clinch River bottom-sediment cores. The program will be used to compare approximately 50 cores which show similar variations. Results of the program will be used for estimating the thickness of radioactive sediment in cores which did not penetrate the full thickness, as well as for measuring the degree of similarity of the distribution of activity in the cores. Cores are being processed at the present time.

Gamma-spectrum analysis has been completed for parts of 11 bottom-sediment cores from the Clinch River. The cores were counted in 2-in. increments in the "core scanner," with the output of the scanner being routed through a multichannel pulse-height analyzer. Spectrum analysis was done with a series of computer programs developed by ORNL personnel. Plots of variations of the major gamma-emitting nuclides with depth in the sediment were among the products of the computer programs. Results of the analyses are currently being studied.

Twenty-three 2-in. segments from two Clinch River bottom-sediment cores have been analyzed for radionuclide content, particle-size distribution, cation exchange properties, mineralogy, and content of selected stable-chemical constituents at laboratories of the U.S. Geological Survey

and ORNL. Results of the analyses have been received and will be examined for relationships between the radionuclide content and the chemical and physical properties of the sediment.

Mineral Exchange Studies. - Two types of ion exchange sites are known to be present on clay minerals. They are sites which originate from isomorphous substitution of a higher-charge cation by a lower-charge cation and sites from dissociation of hydrogen ions of hydroxyls situated at the edges of crystals. The contribution to the total exchange by dissociation of hydrogen between pH 7 and 10 and at NaNO_3 concentrations up to 1.0 M was examined for Fithian illite. The exchange capacity determined in neutral water was 23.4 meq/100 g; this value represents contributions by both isomorphous and dissociation sites up to pH 7. At pH 10 the titration curves revealed an increase of 9% in capacity, and at pH 10 and 1.0 M NaNO_3 the curves showed an increase of 26% due to dissociation of hydrogen. In 1.0 M NaNO_3 and pH 7 the increase was less than 0.5%. Intermediate pH and NaNO_3 concentrations showed intermediate values from those reported above.

Disposal in Deep Wells. - Core drilling was started August 5 on a hole 100 ft plant north (up dip) from the injection well, in line with old well No. 2, now called 150 N. The first of the five test injections contained no radioactive material, and it is not known whether it intersected well 150 N. However, injections 2, 3, and 4 all intersected this observation well and were detected by gamma-ray logging. Injection No. 5, although it consisted of about 200,000 gal, or five times the volume of each of the previous injections, did not intersect well 150 N. Core drilling on well 100 N is now (August 20) down to 983 ft, well below the first injection of simulated waste made at 944 ft, but it has not intersected any of the five test injections. It may intersect one or both of the two fractures made by the earlier water injection tests, although so far no evidence of them has been picked up in the cores or by electric logging.

The cores show that locally the shale is sharply folded, although the individual folds or zones of folding are small (of the order of 2 to 10 ft thick). Some as yet unknown combination of circumstances has deflected all five of the main test injections, and possibly one or more of the water injections, away from the direct up-dip direction sufficiently for them all to have missed the well 100 ft up dip from the injection well; three of the four radioactive sheets, however, intersected the observation well 150 ft up dip. Any attempt at explanation would be premature, but when all seven scheduled core holes have been drilled we expect to have at least a partial answer.

Low-Activity Waste: Pilot-Plant Work. - The scavenging-precipitation portion of the scavenging-precipitation foam-separation process equipment has been operated at 5 gpm for 50 days with tap water and for 25 days with ORNL low-level waste (LLW) as feed. To reduce hardness prior to foam separation, caustic and soda ash are added to make the feed 0.005 M in each, and copperas is added to make the feed 5 ppm in Fe^{2+} . Except for short periods following minor equipment failures, the total hardness of the clarifier effluent was maintained at a satisfactory 3 ppm (as CaCO_3). The strontium decontamination factor ranged from 10 to 15.

The operation of the foam column was stable during preliminary tests, but the foam bubbles produced by using rayon spinnerets for air distribution were larger than the bubbles produced during earlier development tests of similar spinnerets. The foam-recovery system was unstable, with pressure and flow surges occurring continually. After several unsuccessful attempts to correct this without making major equipment changes, it was decided to bypass this system temporarily and perform tests in the foam column with actual LLW as feed.

The foam system was first operated with clarified LLW at 2 gpm, with the feed containing 200 ppm of foaming agent (dodecylbenzenesulfonate). The air flow rate through nine rayon spinnerets was 4 cfm. The decontamination factor for strontium across the foam column was only 4.4 to 9.2 (6.6 av) during a four-day operating period, and about 100 overall for both the precipitation and foam steps. The ratio of feed volume to condensed-foamate volume was 45, and the parameter $VL^{-1}d^{-1}$ (V = air flow rate, L = liquid flow rate, d = bubble diameter) was about 75 cm^{-1} .

Laboratory tests have shown that for significant strontium decontamination, $VL^{-1}d^{-1}$ must be at least 150 cm^{-1} . In a subsequent test, this parameter was raised to between 150 and 250 cm^{-1} by replacing the rayon spinnerets with porous stainless steel spargers to reduce the bubble size. However, the strontium decontamination factor in this test fell to between 2 and 4. It is believed that the difficulties arose from an inadequately sized section of piping which in turn caused liquid to overflow a dam and then channel down the wall of the column.

Low-Activity Waste: Laboratory Work. - In the modified scavenging-precipitation process for decontaminating low-level wastes, phosphates caused abnormally high residual hardness after the scavenging step. Although its capacity for hexametaphosphate (the species most commonly present in detergents) is known to be nil, chromatographic-grade activated alumina (Alcoa F-20) lowered the total phosphate concentration to 1 ppm or less and permitted more nearly complete precipitation of hardness. The high cost of this material (\$1 per pound) provided an incentive for evaluation of more economical grades: Alcoa F-1 (15¢ per pound) and Alcoa H-51 (40¢ per pound). The F-1 material (same surface area as the F-20, $200 \text{ m}^2/\text{g}$) removed 50% or more of the phosphates in 25,000 bed volumes of raw waste, initially containing up to 1 ppm total PO_4^{3-} . The H-51 material ($400 \text{ m}^2/\text{g}$) removed about 5% more phosphates than F-1 during the same period of time and did not fall below 50% removal until about 29,000 bed volumes had been processed. The capacity of F-20 was previously reported to be about 15,000 bed volumes for waste containing up to 3 ppm PO_4^{3-} . On the basis of the performance during processing and the incomplete results of the regeneration of each grade of alumina, it would appear that, economically, the F-1 alumina is the most suitable.

Another decontamination process under study is one in which raw waste is treated by a flocculation and clarification procedure under near-neutral conditions (pH about 7.0) to eliminate the radiocolloids and suspensions and then is treated by either fixed-bed or continuous ion exchange to remove the ionic activity. Previous flocculation conditions have been at pH 11.0 to 12.0. The optimum conditions for clarification are to be determined (1) by measuring the zeta potential of the suspended particles, (2) by neutralizing this charge with the addition of coagulants and coagulant aids so that sedimentation will occur, and (3) by selecting an

appropriate filtering medium to remove the small amount of solids that remain suspended in the aqueous medium. Zeta-potential measurements of samples of raw waste taken over a two-month period indicate a variation of -8 to -16 mv. Preliminary results of beaker tests using alum for coagulation show (1) that clarification is best at about -5 mv rather than zero and that it requires from 6 to 12 ppm of $Al_2(SO_4)_3$; (2) that high-speed flash mixing (1750 rpm) is necessary to ensure efficient encapsulation of the suspended matter by the high-surface-area aluminum hydroxide formed from the alum added; and (3) that coagulant aids such as Grundite clay, activated silica, and organic anionic and cationic polyelectrolytes may be useful in improving the settling characteristics of the fragile alumina floc formed by toughening it and aiding in the growth of floc size.

Low-Activity Waste: Foam Separation. - Two flowsheets for the decontamination of low-level waste by foam separation have been developed: the one- and two-step processes. Several experiments were performed to optimize the two-step process. Problems assessed included the evaluation of different spargers, the testing of square foam columns, the evaluation of biodegradable surfactants, the analysis of waste solutions by fast and economical methods, and the efficiency of removing solids by flotation. All are discussed briefly below.

Four different stainless steel spargers with mean pore diameters of 10, 20, 35, and 65 μ were tested. It was concluded from this study that stainless steel spargers could be used in large-scale foam-separation equipment; in particular, the sparger with 10- μ -diam pores is recommended.

A small and simplified version of the square foam column (4 x 4 in.) used in the pilot plant was tested to provide information on operational conditions with low-level waste. Tests showed that a stable flow regime may be expected. At a feed rate of 400 ml/min, equivalent to a 5-gpm rate in the pilot plant, channeling and flow inversions were observed, as predicted by a model based on perfect foam stability.

Ten biodegradable surfactants were screened for their ability to remove strontium from solutions. Three of them, Igepon-T77, Alipal LO-436, and Nacconel 40FX showed good strontium distribution coefficients (about 0.01 cm^{-1}) and strontium decontamination factors of about 2000 in a countercurrent foam column.

The analysis of spiked low-level waste solutions by the resolution of their gamma-ray spectra according to the method of least squares proved to be a fast and economical method for determining ^{85}Sr , ^{60}Co , ^{137}Cs , ^{106}Ru , and ^{144}Ce content. The determination of surfactant concentration by a fast extraction method, for use in the pilot plant, gave good answers at surfactant concentrations of 0.1 to 2.0 ppm.

Flotation of solids in the foam column takes place together with foam separation. Results of these runs showed that more than 90% of the gross activity is removed by flotation.

In the one-step process, the caustic-sodium orthophosphate precipitant, the ferric ion scavenger, and the surfactant sodium dodecylbenzenesulfonate are all added together in a mixing chamber, and the resulting slurry is fed into a continuous countercurrent foam column. Several variables were investigated to optimize this process, such as contact time in the mixer, flotation agent, surfactant concentration, effect of splitting the foam agent into the foam column, Fe^{3+} and PO_4^{3-} concentrations,

and flow rates. For the optimum conditions, the overall strontium decontamination factor was 250 to 450, with a volume reduction from 12 to 100. It was concluded from a cost-estimation study that the one-step process is not as economical as the two-step process.

Low- and Intermediate-Activity Waste: Incorporation in Asphalt. - Several experiments showed that a sludge simulating one to be derived from the processing of ORNL low-level waste water is easily incorporated into emulsified asphalt. The sludge containing about 18 wt % solids (mainly CaCO_3) was pumped into emulsified asphalt that had been heated to 85°C . The sludge-asphalt mixture was stirred and heated to 190°C to evaporate water and to yield a product sufficiently fluid to flow easily.

The leach rate of ^{137}Cs from a product containing about 60 wt % solids from sludge was $1.3 \times 10^{-4} \text{ g cm}^{-2} \text{ day}^{-1}$ at the end of two weeks. This leach rate is about a third of that obtained with asphalt products incorporating about 60 wt % solids (NaNO_3 - Na_2SO_4 - NaOH) from simulated ORNL waste-evaporator concentrates. Samples of asphalt products incorporating 60 wt % solids from evaporator concentrates have been leached with distilled water for six months. The results show that the leach rate tends to level out at about $4 \times 10^{-4} \text{ g cm}^{-2} \text{ day}^{-1}$.

High-Activity-Waste Solidification: Engineering Work. - The induction-heating furnace was modified so that heat is induced in a 15-in.-diam stainless steel susceptor and is then transferred from the susceptor to the pot, principally by radiation and convection. This modification was necessary because pot failures due to localized overheating and corrosion occurred in previous tests when heat was induced directly in the pot walls.

A calcination test with a simulated Purex waste was made in the modified furnace using an 8-in.-diam pot. In addition to the customary 20 thermocouples associated with the pot, 30 more were used on the susceptor to monitor for "hot spots." The maximum temperature spread on the susceptor was 250°C during heating up and 150°C during steady-state operation. Upon completion of the test, examination of both the pot and susceptor revealed that the only zone of overheating was a narrow (1-1/2-in.-wide) ring, about 3 in. from the bottom of the susceptor. The system was not damaged, however, and will be used in the next test.

Excessive foaming during the test resulted in an average feed rate of only 9 liters/hr, compared with 20 to 30 liters/hr achieved in previous tests with electrical resistance furnaces. The cause of the foaming in this test has not been ascertained.

High-Activity-Waste Solidification: Laboratory Work. - Current developmental work is aimed at incorporating waste in glassy solids suitable for storage in salt or granite formations. Work has continued on optimizing the lithium aluminum phosphate "glasses" for incorporating Purex waste of both sulfate and non-sulfate types, on the development of a laboratory-scale continuous evaporator-melter, and on the corrosion of structural materials for such a melter.

Inclusion in the glasses of elements simulating fission products resulting from processing a fuel irradiated to 10,000 Mwd/metric ton increased the waste oxide content of the final products by 30 to 50% (e.g., from 40 to 52% and from 20 to 30% of the total weight of product). Melting temperatures were generally increased by about 300°C as the result of fission product additions. Decreasing the total content of waste oxides (e.g., from 52 to 30% for a sulfate-containing solid) resulted in solids

melting at 800°C or lower and having sufficient fluidity to permit their production in the laboratory-scale continuous melter. Glasses that incorporated up to 24% waste oxides and that were fluid at 800°C were prepared from simulated non-sulfated Purex waste, including fission products.

Corrosion of the continuous melter increases rapidly with operating temperature but is also markedly dependent on other operating conditions that are more difficult to define. In short-term exposures in the melter, platinum showed no corrosion; Hastelloy F and Inconel showed only slight corrosion; and types 310, 304L, and Carpenter 20 stainless steels and Ni-0-nel showed localized attack of varying degrees. Hastelloy B showed excessive general corrosion.

Disposal in Natural Salt Formations. - The drilling, casing, and cementing of the 1000-ft-deep, 19.1-in.-ID waste-charging shaft have been completed. A deviation survey has shown that the bottom of the hole is displaced 2.5 ft from a true vertical direction.

Work underground on tunnel clearing and ramp building is in progress. It is anticipated that mining of the experimental area will start about September 1, 1964. A new mine-level power distribution system has been installed.

Design of the waste-charging shaft facility is in progress, and bids for part of this work will be requested during September.

After 7 weeks of operation, the prototype test was shut down, and the bottom portion of the hole liner was pulled for inspection. There was no significant corrosion of the liner or associated components and no indication that there will be any major problems associated with this phase of the demonstration. The prototype liner is to be reinstalled, and operation will continue indefinitely to see whether any long-range problems develop.

Engineering, Economic, and Safety Evaluation. - As estimates of total fuel-cycle costs for advanced reactor concepts decline from previous highs of several mills per kilowatt-hour (electrical) to less than 1 mill/kwhr (electrical), the cost of about 0.03 mill/kwhr allocated to waste management becomes increasingly significant. In the light of this fact, and also to establish a basis for comparing the costs of alternative waste-management schemes, a detailed estimate of the costs of "perpetual" tank storage of wastes is being undertaken. Storage of Purex and Thorex solvent extraction raffinates as both acid and alkaline solutions is considered, and storage of Zirflex and Sulfex decladding wastes in alkaline form is postulated. Costs are being developed for use in a computer code that will calculate the total storage costs based on the optimal tank size for a given filling rate and return on investment.

A second collection of fish in the Clinch River and the Tennessee River was completed during 1963. Only bottom feeders (carp, buffalo, and carpsucker) were collected, and the flesh was analyzed for ^{90}Sr and ^{137}Cs . Although the concentrations of both radionuclides in the flesh were found to be less than those observed during the period 1960 to 1962, a "t" test showed that only ^{90}Sr in carp and carpsucker and ^{137}Cs in carp were significantly different at the 5% level. At an assumed rate of fish consumption of 37 lb/year, the estimated fraction of maximum permissible intake attained by eating contaminated fish was less than 0.01 for the critical organs, bone, total body, gastrointestinal tract, and thyroid.

PHYSICAL RESEARCH

PHYSICS AND MATHEMATICS

High-Energy Physics. - The interaction of 3.25-Bev/c π^+ mesons with deuterons in the BNL 20-in. deuterium-filled bubble chamber is being studied. Several thousand events have been measured and are being fitted to reactions that yield two protons, two charged pions, and one or no neutral pions in the final state. The η , ω , ρ , f^0 , and A resonances are clearly observed in the two- and three-pion systems. An extensive analysis is in progress to determine the decay characteristics of the A particle.

Physics of Fission. - Correlated energies and velocities of single fission fragments from the spontaneous fission of ^{252}Cf have been measured. Absolute calibrations of energies and times of flight were obtained with estimated accuracies of $\pm 0.3\%$ from direct comparison measurements with 30- to 120-Mev ^{79}Br , ^{81}Br , and ^{127}I ions from the Tandem Van de Graaff accelerator. The post-neutron-emission kinetic parameters obtained from this experiment have been compared with the pre-neutron-emission quantities obtained from double time-of-flight experiments. Of special interest is the fine structure which appears in the present post-neutron-emission mass distribution. It is shown that this structure reflects the fine structure observed in the pre-neutron-emission mass distribution, which in turn reflects certain energetically preferred even-even fragment configurations in ^{252}Cf spontaneous fission. Within the $\sim 2.5\%$ mass resolution of the present experiment, no additional fine structure appears as a result of neutron boil-off to specific fragment masses. The number of neutrons, $\nu(M)$, as a function of fragment mass has been calculated from the pre- and post-neutron-emission mass distributions.

High-Voltage Experimental Program: Construction of a General Purpose Scattering Chamber for Charged-Particle Spectrometry. - An 18-in.-diam, general purpose, high-precision scattering chamber has been constructed and placed in operation at the tandem accelerator. As the entire top of the scattering chamber is removable, and as there is a 9-in. port in the bottom, the chamber is adaptable for a variety of apparatus to meet different experimental conditions.

The present chamber fittings have been designed for use with an array of solid-state detectors. In order to retain the high resolution possible with these counters, while keeping the preamplifiers accessible, the detectors are suspended from the chamber top. The detector angle is then varied by rotating the chamber top. Because the detector mounts are inserted through holes in the top, they can be quickly removed or replaced. Pins in the lid allow the counters to be accurately positioned. A total of 29 such holes, with a choice of two radii, at 3.5 in. and 7.0 in., are provided. The top can be remotely rotated, and the angular setting can be read on a vernier with an accuracy of better than 0.1° .

The targets are mounted on a rod which can be moved vertically in order to place different targets in the beam, as well as rotated about its axis. The target holder is insulated from the scattering chamber so that the targets may be biased to reduce secondary electron emission.

A cold trap, requiring filling about every 12 hr, is located at the 9-in. port in the chamber bottom. This large, cold surface minimizes target contamination and gettering of pump oil by cooled detectors. A vacuum of about 2×10^{-7} mm Hg is obtained in the chamber, with no observable pressure rise as the top is rotated.

The chamber is presently being used for studying nuclear reactions by use of counter telescopes, as well as for inelastic scattering experiments.

High-Voltage Experimental Program: Gamma-Ray Spectroscopy with Lithium-Drifted Germanium Detectors. - During the past two years a significant tool, the lithium-drifted germanium solid-state detector, has been developed for the study of gamma rays. Its importance results from its improved resolution over the conventional NaI crystal gamma-ray detector. We have acquired two of these detectors which yield a width of 3.7 keV for the ^{51}Cr 320-keV gamma-ray line. This is to be compared with a width of 30 keV obtained by means of an NaI crystal. The gamma-ray spectra of ^{102}Rh , ^{106}Rh , and ^{110}Ag have been investigated with these solid-state detectors. A pair of previously unresolved peaks were observed in the spectra of both rhodium isotopes. In ^{102}Rh the energies of the doublet are 631.6 ± 0.5 and 628.1 ± 0.7 keV, and the ratio of their intensities is 10 ± 2 . In ^{106}Rh the energies are 622.2 ± 0.5 and 616.2 ± 0.9 keV, and the ratio of their intensities is 14 ± 2 . The detectors have also been used to establish better energy values of several standard gamma rays. They are (in keV): ^{51}Cr , 319.8 ± 0.4 ; ^7Be , 477.3 ± 0.3 ; ^{54}Mn , 835.4 ± 0.7 ; ^{65}Zn , 1114.8 ± 0.5 ; ^{22}Na , 1274.2 ± 0.5 ; ^{88}Y , 1836.6 ± 0.8 .

Nuclear Data. - Volume 6, Set 1, of Nuclear Data Sheets was completed in August. This contains up-to-date analyses of nuclear properties of 30 nuclei - those with mass numbers 162, 163, 164, 167, and 169.

For several years we have collected all data relevant to accurate nuclear mass determinations. In February, we borrowed a computer program to organize these data and to determine best mass values. It has taken six months to get the program working and adapted to our needs. Set 1 contains the first group of usable results from this program.

A four-year project of compiling and analyzing nuclear magnetic moments was completed in August and will be published later this year.

Work continues on analyzing nuclear data. Presently, nuclei of mass numbers 166, 168, 170, 171, 172, 173, and 174 are being studied. A collection of Recent References (organized by nucleus) to papers prior to July 1964, but not yet included in the Nuclear Data Sheets, is being prepared. We are currently adding key words to the galley proofs of articles to be published in the journal Nuclear Physics.

Medium-Energy Nuclear Physics: Experimental. - Deuteron spectra were measured at ten angles for the reaction $^{89}\text{Y}(p,d)^{88}\text{Y}$ produced with 19-MeV protons from the ORIC. The proton beam was obtained by accelerating H_2^+ ions to 38 MeV. Silicon surface-barrier detectors were used for both E and ΔE counters. The data were recorded on the 20,000-channel pulse-height analyzer. The statistical fluctuations in the energy loss of the

deuterons in the ΔE counter can be seen clearly in the ΔE by E data array; the monoenergetic groups of deuterons appear as tilted lines instead of round spots in the array. At least six levels were resolved at low excitations. In the analysis of the data, we will attempt to assign the observed levels to those levels expected from the $p_{1/2}$ - $g_{9/2}$ neutron and proton shell-model configurations. The reaction should excite some, if not all, of the eight levels, two each at spins 0^+ , 1^+ , 4^- , and 5^- , for which wave functions can be constructed to have nonzero spectroscopic factors for $p_{1/2}$ or $g_{9/2}$ neutron pickup from ^{89}Y . All these states are pure $T = 5$ except one of the 0^+ states, which is $T = 6$; it should occur at a much higher excitation (~ 7 Mev) than the $T = 5$ states.

Medium-Energy Nuclear Physics: Experimental, Polarized Protons. - A secondary beam of polarized protons, produced by an alpha-particle beam on a hydrogen target, is now available in the ORIC. With a primary beam of $10 \mu\text{a}$ of 80-Mev alpha particles, the polarized-proton beam produced by (α, p) elastic scattering at a laboratory angle of 25.5° has the following properties:

Proton energy	40 Mev
Energy spread	1.5 Mev (fwhm)
Beam intensity	2×10^7 protons/sec
Beam spot size on secondary target	0.3 in. wide by 1.1 in. high

With the above beam, the asymmetry in elastic scattering of the protons was measured in the angular range from 10 to 140° for a ^{12}C target, and from 10 to 110° for ^{40}Ca and ^{208}Pb . The results for ^{12}C represent an extension of data obtained elsewhere to both smaller and larger angles; the regions of data overlap appear to be in fair agreement, if the polarization of our beam is assumed to be about 90%. In addition, asymmetry in inelastic proton scattering from two excited states of ^{12}C and two excited states of ^{40}Ca was observed.

Medium-Energy Nuclear Physics: Theory. - The binding energies of the nickel isotopes were calculated following Talmi's method of "effective interactions" in which the isotopes are considered in two groups: (I) $^{28}_{28}\text{Ni}_{29}$ to $^{60}_{28}\text{Ni}_{32}$ in which the neutrons are filling the $2p_{3/2}$ shell, and (II) ^{61}Ni to ^{66}Ni in which the neutrons are filling the $1f_{5/2}$ shell. The binding energies of the isotopes in group I (group II) are determined by the binding energy $\epsilon_{3/2}$ ($\epsilon_{5/2}$) of a single $2p_{3/2}$ ($1f_{5/2}$) neutron to the ^{56}Ni (^{60}Ni) core and by the energy matrix elements for the effective residual interactions between two $2p_{3/2}$ ($1f_{5/2}$) neutrons. The matrix elements $E_J = \langle (p_{3/2})^2 J \neq 0 | H_{nn} | (p_{3/2})^2 J \neq 0 \rangle$ and $E_J = \langle (f_{5/2})^2 J \neq 0 | H_{nn} | (f_{5/2})^2 J \neq 0 \rangle$ are obtained from the spectra of ^{58}Ni and ^{62}Ni . The single-neutron binding energies and the matrix elements E_0 are regarded as free parameters and are determined by a least-squares fit to the binding energies of the ten isotopes. The binding energies of the isotopes in groups I and II are reproduced to better than 270 and better than 200 keV respectively.

Although configuration mixing is expected to be quite significant for nuclei in this region, the present calculation indicates that a reasonable estimate of the binding energies might be possible if one uses effective interactions within a single shell. Calculation of the binding energies for nuclei having both protons and neutrons in the $2p_{3/2}$ and $1f_{5/2}$ shells is in progress.

Cyclotron Operations. - In the continued operation of the ORIC on a 14-shift/week schedule, the reliability of cyclotron operation and the stability of the extracted beam have met all expectations. During this period the cyclotron was scheduled for nuclear physics bombardments about 68% of the total time. Beams of ~36-Mev protons, ~81-Mev alpha particles, or ~37-Mev deuterons were supplied to various target positions in the small experiment room. About 20% of the scheduled time was assigned to cyclotron improvement and development studies, and the remaining 12% was taken up with the continued installation of various control circuitry. The beam was "on target" about 62% of the total time scheduled for nuclear physics work.

Medium-Energy Electronuclear Machines. - A modest program was undertaken to correlate the experimentally determined main-magnet and trimming-coil current settings for the ORIC with those calculated from the original magnetic field measurements. These original measurements were corrected to agree with a series of field measurements made recently with a nuclear magnetic resonance fluxmeter. The new current settings, computed from the new trimming-coil data via linear programming, are now consistent with experimentally determined values. We now believe that the computer system, along with phase slip measurements from the cyclotron, can be used via successive approximation to optimize ion dynamics in the cyclotron and to improve performance.

An immediate result of the magnetic field studies was the determination that an 8-in.-diam depression in the center of the ORIC magnetic field cannot be satisfactorily compensated by the trimming coils. The depression is sufficient to cause axial loss of beam, especially for particles out of phase with the rf voltage. The result is a decrease in phase acceptance of the cyclotron, which could be an undesirable limitation in some future experiments. To eliminate this depression in the field, small pole tips are being designed for the center of the cyclotron. These will be remotely positioned to permit optimum correction over the whole range of magnetic fields encountered for various particles and energies.

The electrostatic deflector channel now used in the ORIC was designed to obtain preliminary information for the final design. This channel has proved to be satisfactory in principle but to lack the desired mechanical stability. An improved deflector was designed and is being fabricated.

The 153° beam analyzing magnet is now assembled, and field measurements are being made before it is installed. A purchase order for an Elbeck-type broad range spectrograph was placed with Spectromagnetics; some of the fabrication drawings are now being reviewed.

Electronuclear Systems. - The rf power required in a 200-800 Mev section of a separated-orbit cyclotron (SOC) can be reduced by at least

a factor of 0.65 by designing the cavity so that the rf voltage varies with radius, increasing up to 1 Mv rather than remaining constant at that value at all radii. At the input radius a value of only 200 kv is sufficient to give the desired 4-in. turn separation. The shape, construction tolerances, and tuning details of the cavity are being determined. The mechanical structure is partially designed.

To determine the best type of magnetic focusing to use in the guide field of an SOC, it has been necessary to evaluate the relative stability limits, acceptance, and sensitivity to misalignment errors of the possible focusing configurations. The choice is between a series of doublets (OFDOFDO...) and triplets (OFDDFODFFDO...). Acceptance values greater than 20 mm-milliradians at 200 Mev into a 1-in. aperture are possible with radial or axial alignment tolerances up to ± 9 mils for a single pole tip. This tolerance, which allows a 0.5-in. peak-to-peak growth in betatron oscillations, includes both the bench alignment errors of the pole tips in a lens and the relative alignment errors of the lenses to each other. The matching of the acceptance and emittance of the deflection sector to that of the adjoining normal sectors is of particular concern. We find that solutions are possible with an open space of up to ~ 3 m in the deflection sector.

CHEMISTRY

Protactinium Chemistry. - The bulk of the ^{231}Pa borrowed from England for use in preparing ^{232}U has been returned. Since the amount of material recovered from the protactinium purification processing was somewhat less than expected, we examined various wastes from the processing solutions and equipment for any additional protactinium. At most, a few hundred milligrams of protactinium is contained in them. Most of this material has been recovered and purified.

The equipment used for the initial ^{232}U recovery, made more than two years ago, was exhumed from the burial ground, and two resin columns and the dissolver vessel were recovered. The resin columns now give radiation readings of about 1 r/hr, indicating that they do not contain any large amount of protactinium. However, the dissolver gives readings of over 100 r/hr at the bottom, and such a high rate might indicate a significant amount of protactinium. These items will be processed for protactinium recovery as soon as hot-cell space becomes available.

Transport Properties of Gases: Pressure Dependence of Thermal Diffusion. - The pressure dependence of thermal diffusion has been derived on the basis of the "dusty-gas" model, in which a porous medium is considered as a collection of giant molecules (dust particles) fixed in space. The results can also be applied to capillaries by suitable substitution for geometric parameters.

The results correctly predict that thermal separation is zero at zero pressure and constant at high pressures; but they yield a quite complex and varied transition between these two limits which depends upon the temperature, molecular masses, and intermolecular forces of the gas molecules involved. Representative calculations illustrated the possibility of maxima and sign reversals of the thermal separation as a function of pressure. A detailed report of this work is to be issued shortly.

Transport Properties of Gases: Gaseous Diffusion. - The gaseous diffusion program is oriented toward two objectives: (1) to provide values of the gaseous diffusion coefficient, accurate within about 2%, for binary gas systems in the temperature range 0-120°C; and (2) to determine parameters characteristic of the interaction potential of the molecules involved. The apparatus has been calibrated with the helium-argon system and thus far has been used to determine the diffusion coefficients of the helium-xenon and argon-xenon systems over the range of temperature cited. Although the argon-xenon results are in satisfactory agreement with values reported by other workers, the data obtained for the helium-xenon system are about 5% lower than previously reported values, but in good agreement with diffusion coefficients which have been estimated from the composition dependence of the viscosities of helium-xenon mixtures.

Analysis of Molten Salts by Electrochemical Methods: Voltammetric Measurements in Molten Fluoride Salt Systems. - A reference electrode similar to the one used by Steinmetz (UNC-5032) was prepared. This electrode consists of an intimate mixture of powdered nickel and nickel(II) oxide contained in a zirconium oxide tube. Contact with the Ni-NiO mixture is made with a nickel wire. When the electrode is immersed in the melt, the ZrO₂ becomes a solid ionic conductor (oxide ion membrane) and thus serves as the salt bridge. The electrode is supposedly a second-order electrode which is stabilized by the oxide ion activity in the solid mixture of Ni and NiO at 500°C.

The cathodic limit of the molten mixture of LiF and BeF₂ vs this new reference electrode was essentially constant at -1.8 ± 0.02 v for 3 weeks; apparently this limit is unaffected by whether the helium cover gas is static or flowing, unlike the case previously observed (ORNL-3663, pp. 24-25) for the platinum quasi-reference electrode. This new electrode also appears to be better poised than the platinum one in the same molten mixture.

Tests were made in which the current-voltage curves of the system were recorded with the Ni-NiO reference electrode in the circuit, and the potential of the nickel reference electrode was monitored vs a platinum quasi-reference electrode (1-mm-OD platinum wire immersed in the melt). The potential difference between the nickel reference and platinum quasi-reference electrodes did not deviate more than ± 0.01 v throughout the range of the current-voltage curve. The cell current ($\sim 10^{-11}$ amp) which flowed in the reference circuit of the controlled-potential polarograph did not polarize the nickel reference electrode. Larger currents, however, did affect the electrode; for example, 10 μ a flowing through the cell caused the potential to change by ~ 0.05 v. In an effort to improve the current-carrying capacity of the nickel reference electrode, the dry Ni-NiO mixture inside the ZrO₂ ceramic tube was replaced with LiF-BeF₂ melt which contained an excess of NiO (5% by weight) so as to form a saturated solution of nickel oxide. This did not significantly improve the electrode in terms of current-carrying capacity; however, the resistance of the electrode decreased from ~ 18 kilohms to about 6 kilohms. This in itself appeared to improve the general operating characteristics of the reference electrode when used in a three-electrode controlled-potential circuit.

It appears at this stage that this type of electrode will serve as a useful reference electrode for molten-salt voltammetry when utilized in a three-electrode controlled-potential circuit. It could not, however, be used safely in a two-electrode circuit, because the cell current which flows through the reference electrode under these conditions would possibly lead to polarization and subsequent erratic potential values.

Spectrophotometry of Solutions over Wide Ranges of Temperature and Pressure. - We reported (ORNL-3628) measuring the absorption spectrum of CO₂ in the condensed state between 1.19 and 1.66 μ as a function of temperature from -80° and 13 psia to 65° and about 2000 psia. More recently we reported (ORNL-3679) fitting the combination bands, (ν₁ + 4ν₂ + ν₃) and (2ν₁ + 2ν₂ + ν₃), over the entire fluid range by Lorentz functions. The molar absorptivities of these two band maxima (ε_{max}) decrease line-

arly with temperature from the freezing point (fp), -56.6°, to the critical point (cp), 31.1°. The decrease amounts to -0.6%/°C at the fp for both bands and is qualitatively different from the temperature dependence of the overtone and combination bands of liquid NH₃ (+0.16%/°C at the fp); H₂O (+0.6%/°C at the fp); and D₂O (+0.6%/°C at the fp).

The integrated intensities ($\int_{-\infty}^{\infty} \epsilon \, d\nu$) of the CO₂ bands, (ν₁ + 4ν₂ + ν₃) and (2ν₁ + 2ν₂ + ν₃), in contrast with their ε_{max}, increase nonlinearly with temperature, from ~0.2%/°C at the fp to ~5%/°C as the cp is approached.

The half-intensity bandwidth for a Lorentz band varies as the mean collision frequency, which in turn increases with increasing fluidity. Hence one might expect for these CO₂ bands a simple relation between bandwidth and fluidity. Indeed, Δν is proportional to the fluidity from the fp to within 10° of the cp.

TRANSURANIUM-ELEMENT PRODUCTION

Chemical Process Development: Separations. - The anion exchange behavior of curium, californium, and einsteinium with nitrilotriacetic acid (NTA) was investigated. Adequate separations were not obtained in this system. Separation factors for Cm/Cf and Cf/Es were 1.14 and 1.06 respectively. The elution order was: Cm; Cf; Es.

The anion exchange behavior of α-hydroxyisobutyrate complexes with curium, californium, and einsteinium was investigated. We saw no indication that this system provided a separation scheme but did find evidence of the formation of Me(Y)₃⁰, Me(Y)₅²⁻, and Me(Y)₆³⁻ complexes (where Me is the metal and Y is α-hydroxyisobutyrate). The dissociation constants for the four complexes were calculated to be: pK₁ = 3.46, pK₂ = 2.71, pK₃ = 3.68, and pK₄ = 4.54. The first anionic complex is unstable with respect to Me(Y)₃, and all anionic complexes of α-hydroxyisobutyrate are formed in very small quantities.

Equipment which will be operated in cell 3, Building 4507, is being set up for the separation of gram quantities of ²⁴³Am and ²⁴⁴Cm. Two

systems will be studied: (1) LiNO_3 anion exchange and (2) oxidation of americium to Am^{5+} followed by precipitation as $\text{K}_3\text{AmO}_2(\text{CO}_3)_2$. The LiNO_3 anion exchange system is being cold-tested. Apparatus for the alternative system will be completed soon.

Chemical Process Development; Sol Preparations. - Since the sol-gel technique would provide a convenient scheme for the preparation of PuO_2 suitable for HFIR targets, efforts to develop this method have continued. One problem being investigated is that of accurately determining the nitrate concentration of plutonium sol preparations; present indications are that micro-Kjeldahl analysis for nitrate is the most reliable procedure investigated to date. Plutonium sols have been prepared in which the nitrate concentration is as low as 0.08 to 0.13 mole of nitrate per mole of plutonium. Sphere-forming equipment was installed in a glove box, and the operating variables of this equipment are presently being investigated with thoria sol. Attempts will be made to produce and characterize gram quantities of plutonia spheres.

Investigations of lanthanide sols, which are suitable stand-ins for americium and curium sols, have continued. A successful sol-gel procedure could be useful for the preparation of americium and curium oxides in a desirable particle-size range for HFIR recycle targets. Recent analyses of lanthanide preparations indicate that adsorbed atmospheric CO_2 may have prevented good sol formation. The most favorable-appearing preparation to date was made by electrolysis of gadolinium from a nitrate solution through a cation membrane into the cathode compartment, which contained water. The sol that formed in the cathode compartment was concentrated by evaporation and then used to prepare microspheres that retained their shape after calcining at 1000°C . However, the spheres were very fragile, and microscopy revealed surface imperfections.

Curium Recovery Facility. - Cells 3 and 4 in Building 4507 are being equipped to test transuranium process chemistry at full-scale radioactivity levels and to recover gram quantities of ^{242}Cm and ^{244}Cm . Operations during this report period include continued equipment modification, leak testing, and flowsheet testing.

The replacement of polyethylene lines with suitable metal ones is nearly complete, and all tanks have been reinstalled. The revised piping is being leak-checked. Construction of the Zircaloy-2 mixer-settler rack and scrubber rack was finished. The reworked tantalum-plated tank appeared to be satisfactory during initial testing; this tank has been installed in the cell for further testing. Zircaloy tubing in the evaporator overhead catch tank was severely pitted in the vicinity of welds by HCl-HNO_3 fumes and solution; this tubing was replaced with tantalum tubing. Previous corrosion studies had indicated that Zircaloy-2 was probably not satisfactory for such service; and, in the future, tantalum will be used for all elevated-temperature applications. Two of the new, hardened, disconnect bolts have broken at a sharp-edged relief, apparently without undue strain. It is believed that stress concentration during heat treatment was responsible. The remainder of the bolts will have a radius at the point of fracture. The CRL heavy-duty extended-reach manipulators have been installed and tested.

A laboratory-scale flowsheet test of a modified Tramex fuel solution (0.67 M AlCl_3 -8 M LiCl) with a mixed nitrate-chloride amine extractant was made. The higher aluminum concentration would permit simpler feed adjustment, while the mixed nitrate-chloride amine extractant should compensate for the lower salt strength of the feed. Since the normally used nickel is not a suitable stand-in for actinides in nitrate systems, final testing of this flowsheet must await "hot" operation.

Process Equipment Development: Cell Mockup. - The modified version of the double booting for the heavy-duty, extended-reach manipulators was installed easily with the modified tools. Performance of the manipulators with this booting was good, considering the weight of double booting. The only real problem concerns the seal-ring fastened to the boot. This ring was pulled from the through-tube during installation and had to be replaced by hand. The following changes should solve this and other minor problems: (1) the seal-ring design must be improved to give better gripping action; (2) sharp corners that contact the boot on the seal-ring and the installation tool must be rounded; and (3) a blank through-tube seal plate would permit slight air pressure application to the boot before installation on the manipulator.

Two disconnect clamps of the final design were checked for clamp-arm misalignment at 60 lb-ft of torque. Misalignments of 1.3° for clamp 31 and 1.2° for clamp 25 were measured along a line intercepting the center line of the clamp bolt and the center line of the disconnect. Misalignments of 0.7° and 1.0° were measured 90° to the above line. The rake angle that compensates for this misalignment will be increased slightly for the remainder of the clamps, and the misalignment will be routinely checked on 10% of the production run.

A test was made of the compression force necessary to deflect 1/4-in.-thick sponge-rubber gasket material on the absolute filters being tested. A force of 900 lb produced a deflection of 0.164 in.; 600 lb produced 0.139 in.; and 300 lb produced 0.100 in. of deflection. The gasket was 3/4 in. wide and fastened to a filter box 2 ft square. The deflections given above represent the combined deflections of the gaskets on each side of the box.

HFIR Target Fabrication Development. - Metallography of the first target prototype has been completed at Vallecitos. The polishing and etching results were not comparable with those for unirradiated material and did not show the aluminum grain substructure clearly enough for accurate temperature estimations. The structure, however, clearly showed that there was no melting. Evidence of a possible reaction of the aluminum matrix with the PuO_2 is indicated. If such a reaction occurs, it would be similar to that observed in irradiated UO_2 dispersions in aluminum. The larger oxide particles exhibited significant internal porosity. There appears to have been a decrease in the void spaces in the aluminum matrix. A more detailed evaluation will be made when the specimens can be examined in the HRLEL and compared with the unirradiated control. Fission-gas and burnup analyses have not yet been completed.

Transuranium Facility Design and Construction. - Erection of the concrete shielding walls for the Transuranium Processing Plant cell bank is rapidly being completed. All peripheral walls are at final height,

except for about 16 in. of the front wall and the rear walls of cells 8 and 9. Pouring of the intercell walls can be continued upon receipt of the intercell pass-through ports. Installation of the conveyor housing was completed after some difficulties were encountered in obtaining the flatness and alignment required. Special housing ring adapters were designed for immediate fabrication to alleviate the problem of aligning the cubicle floor pans on the conveyor housing. The cubicle-floor pans and stainless steel gate valves were received and delivered to the contractor. Upon receipt of the stainless steel globe valves, expected in early September, the entire complement of ORNL-furnished materials will have been provided to the contractor.

Design of the chemical process equipment, scheduled to be 84% complete, is 9% behind schedule but should be completed on schedule in February 1965. Fabrication in the ORNL shops of the major portion of this equipment is proceeding on a schedule calling for completion by July 1, 1965. Fabrication in the ORGDP shops of about 20% of the equipment will be started September 1 and completed next May. Some minor delays still result because of a shortage of disconnect clamps. The clamps are now being produced at the rate of about 250 per month.

Corrosion. - Welded Zircaloy-2 specimens exhibited excellent corrosion behavior in an oxygenated hydrochloric acid and organic mixture at room temperature and at 43°C. In each case, the well-agitated mixture consisted of equal volumes of 8 M HCl and 30% Alamine 336 chloride in diethylbenzene. Solution- and vapor-phase corrosion rates after 1000-hr tests were appreciably less than 0.1 mil/month. There was no evidence of localized attack on any of the specimens.

Zirconium containing 1% platinum showed poor resistance in boiling and oxygenated 6 M HCl-0.1 M HNO₃ solution; a corrosion rate of 17 mils/month was obtained after 500 hr of exposure. Zircaloy-2 corroded at a rate of 2 mils/month after 500 hr in the same environment.

Specimens of Homolite CR-39 were exposed in the solution of and the vapor of oxygenated 6 and 8 M HCl solutions at 55°C. Behavior was poor in both environments. After 300 hr in 6 M HCl, solution and vapor specimens showed weight losses of 31.2 and 11.2% respectively. A 200-hr test in the 8 M HCl produced weight losses of 65.6 and 33.3% for solution- and vapor-exposed specimens respectively. All specimens had gummy surfaces immediately upon removal from the test.

METALLURGY AND MATERIALS

Research and Development on Pure Materials. - An attractive method for single-crystal growth is pyrolytic deposition from the vapor phase, because purity of the reactants is easily controlled and production of crystals of very high perfection has already been demonstrated. Recently we grew well-faceted UO₂ crystals (about 0.5 mm on an edge) by passing a gaseous mixture of UF₆, CO₂, and H₂ over a hot platinum filament. We are working to perfect this technique.

Our discovery of the lanthanide germanomolybdates (ORNL-3561, p. 39) led us to expect an analogous series of lanthanide germanotungstates, since Mo⁶⁺ and W⁶⁺ have nearly equal radii. Verifying this, we have grown both Er₂GeWO₈ and Y₂GeWO₈ from Na₂O·2WO₃ at 1150 to 1250°C by a thermal-gradient technique.

We are investigating the use of superconducting magnets for susceptibility measurements. A computer program developed by the Thermonuclear Division is being used to find a coil geometry to produce a magnetic force that is constant over an appreciable volume and at least 100 times the force attainable with ordinary electromagnets. The results to date appear promising and indicate that a single coil with short axial length and large radial depth is best.

Deformation in Crystalline Solids. - We are determining the effect of alloying additions on the low-temperature deformation parameters in body-centered cubic metals. The differences between the activation energies and volumes of the metal and those of a solid solution of the metal would be small if the rate-controlling mechanism were the formation of a double kink over the Peierls stress barriers. The main reason is that the Peierls stress, which would be a major factor in determining the activation energy and volume, is, to a first approximation, a linear function of the shear modulus. Small alloying additions result in only a slight change in the modulus.

We used tantalum and tantalum-base alloys. The activation energies and volumes were measured by differential-temperature and strain-rate techniques. The addition of tungsten decreased the activation energy at a given stress but increased the modulus approximately 2%. However, the activation energy of Cu-10 at. % Al at zero effective stress is four times that of pure copper. The activation volumes at zero effective stress are 70×10^{-22} and 25×10^{-22} cm³ for tantalum and Ta-9.1 at. % W respectively. At an effective stress of 16 kg/mm², the activation volume is 5×10^{-22} cm³ for Ta-9.1 at. % W and 2.8×10^{-22} cm³ for tantalum.

Fundamental Research in X-Ray Diffraction. - As a part of our continuing program of study of short-range order in copper-rich copper-aluminum alloys, we have recently attempted to measure the diffuse x-ray scattering associated with the state of order in a 4% alloy. Although this alloy is far more dilute than any previously studied, preliminary measurements indicate that there is measurable short-range-order diffuse scattering, that it is distributed in reciprocal space similarly to but not identically with that from more concentrated alloys, and that there are important atomic displacement modulations of the diffuse intensity. Precise measurements, useful for quantitative interpretation, are now being made. These measurements require special care and techniques somewhat different from those usually employed for more concentrated systems, since the diffuse intensity of interest is much smaller compared to temperature-diffuse scattering and Compton scattering.

Reactions at Metal Surfaces. - Our previous studies of the oxidation of copper single crystals in the thin-film range indicated the importance of paths of easy diffusion through the oxide in determining the rate of oxidation of copper. To test the generality of this result, we have extended these investigations to the oxidation of single crystals of nickel, silver, and dilute alloys of nickel and aluminum in copper.

Preliminary results with nickel are consistent with the conclusions from our copper oxidation studies. The oxidation characteristics of nickel, like those of copper, were found to be very sensitive to the

presence of surface impurities, and reflection electron-diffraction patterns showed that the oxide on the most rapidly oxidizing planes was much less well oriented than that on the slow-rate planes.

Electron microscopy and diffraction studies showed that the morphology of the oxide formed on a silver single crystal in 1 hr at 150°C under 1 atm oxygen pressure varied greatly with crystallographic orientation. On some planes the oxide appeared to form as discrete nuclei connected by at most an exceedingly thin layer of oxide.

The addition of as little as 1/4 at. % nickel or aluminum produced significant changes in the oxidation characteristics of copper; however, we have not yet established whether these changes are related to an alteration of the paths of easy diffusion in the oxide or to some other factor.

Spectroscopy of Ionic Media. - As part of our continuing study of the spectroscopy of ionic liquids, we have measured the ultraviolet absorption spectra of the isoelectronic ions Tl(I), Pb(II), and Bi(III) in the molten LiCl-KCl eutectic salt. Transition energies for Tl(I) and Pb(II) in the melt are strikingly close to the values for these ions substituted at K^+ sites in crystalline KCl. Consequently, we assign these absorptions, within the context of the tight-binding model, to the $^1S_0 \rightarrow ^3P_1$ component of the $6s^2 \rightarrow 6s6p$ orbital transition. Profiles of these bands yield evidence of strong interactions due to asymmetric arrangements of chloride ions about Tl(I) and Pb(II) in the melts.

Two bands observed in the spectrum of Bi(III) were in general accord with expectations for the $^1S_0 \rightarrow ^3P_1, ^1P_1$ components of $6s^2 \rightarrow 6s6p$. This observation is particularly interesting because there is very little previous information on the excited states of Bi(III) coordinated to halide ions.

Theory of Alloying. - Further studies of the low-temperature specific heats of zirconium-niobium alloys show that, contrary to our earlier report, two superconducting phases appear to be present in alloys of 2 to 4 at. % niobium annealed at 600°C. One of these phases, presumably the omega phase, has a critical magnetic field considerably greater than 21 kilogauss and a critical temperature well above 4.6°K. The other phase, based on alpha zirconium, has a critical field of about 3 kilogauss and a critical temperature that varies from 0.5°K for pure zirconium to 2.7°K for 3% niobium. We believe that only the alpha phase is present in the alloys quenched from the cubic region. With additions of niobium, the alpha phase is characterized by sharp increases in both the density of electronic states and the superconducting transition temperature, a sharp decrease in the Debye temperature, a nearly constant Bardeen-Cooper-Schrieffer superconductivity interaction parameter, and little change in resistivity. Useful technological properties may be found for the high-field minor phase that appears in these alloys when they are quenched and then annealed at 600°C.

In a new zone-refining apparatus we prepared high-purity single crystals of zirconium with the highest resistivity ratio (800) yet reported for this metal. We studied impurity concentrations (as measured by the resistivity ratio) as a function of distance and found that evaporation of impurities was the main purifying effect; however, a small

superimposed concentration profile from zone refining did occur. These zone-refining effects are dominated by impurities that raise the melting point.

Fundamental Investigation of Radiation Damage in Solids: Near-Ultraviolet Luminescence in Potassium Iodide. - Previous studies of the scintillation process led to the suggestion that the near-ultraviolet emission characteristic of all "pure" alkali iodides arises from the recombination of an electron with a self-trapped hole to produce an exciton. Experiments have been performed with KI to test this hypothesis. When KI crystals containing thallium are irradiated at low temperatures with 1.5-Mev electrons, they exhibit absorption bands due to self-trapped holes (V_K centers) and F centers. Illumination of an irradiated crystal with 0.4- to 1.5- μ light results in emission of the 375-m μ band characteristic of the pure crystal and the 425-m μ Tl⁺ emission. Thermal destruction of V_K centers results in complete attenuation of the 375-m μ band. The excitation spectrum exhibits a peak in the F-band region which is attenuated upon optical bleaching of the F band. It is concluded that optical excitation releases electrons from F centers or other (shallow) traps, some of which recombine with V_K centers to produce the 375-m μ emission. Furthermore, V_K centers can be bleached at helium temperature and a new emission band at 345 m μ occurs upon optical stimulation.

CONTROLLED THERMONUCLEAR RESEARCH

The DCX-2 Injection-Accumulation Experiment. - During much of this period DCX-2 has been inoperative because of continued difficulties with the high-voltage power supply, the injector, and the coils. Vacuum difficulties were encountered in trying to use the new injector, and the main container had to be remade. The old injector, when replaced, had an internal water leak; this necessitated reassembly. After many months of use, a short in the east mirror coil, which was found in the early test, suddenly opened, and a deliberate short had to be added to produce the desired field conditions in which the large plasma densities have been observed. Replacement of diodes in the power supply was completed, and the voltage modulation was reduced from ~60 to ~12 kv. Advantage was taken of the downtime to study some of the properties of the lithium arc in DCX-2. The arc density is $\sim 5 \times 10^{13}$ ions/cm³ (within a factor of 3), the electron energy is ~40 ev, and the ion energy is ~15 to 20 ev. Two short runs were made at the end of this report period, and at least one significant result has emerged. After optimization of the field as described previously, the energy distribution of the particles trapped in the plane nearly perpendicular to the magnetic axis shows a considerably higher mean energy than the particles in the groups which spiral more nearly at the pitch angle of the beam relative to the magnetic axis. Further, the axial velocity of the particles at this angle appears to be nearly constant, independent of the total energy of these particles. The machine is now back in normal operation with several new diagnostic tools, and we hope to be able to present new information about the plasma properties in the next report.

Active and Passive Stabilization of Plasmas and Ion Beams. - It is assumed that progress of the DCX program is related directly to the ability to achieve stabilization of the wrapped-up beam. In many respects the calutron ion beam presents a simplified but similar ion beam configuration, and it may be that treatments which improve calutron beams can be adapted (even though not fully understood) to the solution of DCX problems.

The standard calutron used in isotope separation exhibits regions of unstable operation. Increase in ion-beam current decreases the region of stable operation, as does the presence of more than one ion beam.

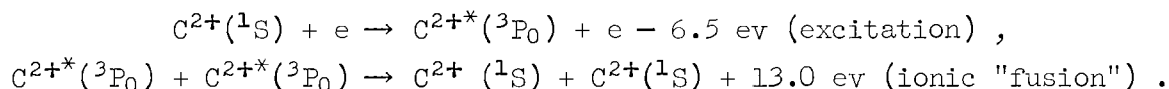
The region of stability can be extended by use of flat plates placed near the ion beam or extended even further if the plates are segmented and electrically isolated by an impedance to ground.

In practice, the use of plates and segmented walls has resulted in a single ion beam of 250 ma which maintains focus and stability at pressures down to 3×10^{-7} torr--the base pressure of the particular system.

Two calcium ion beams of 150 ma each have been run at pressures of 10^{-6} torr with no interference between beams and no defocusing due to reduced pressure. Without wall treatment, beams of this intensity and quality are unobtainable.

Properties of Vacuum Arcs. - Measurements of the ion current to a Langmuir probe located 7/8 in. outside the core of the deuterium arc indicate that the anomalously large transport of plasma across the confining magnetic field by flutes can be essentially eliminated. This arc is normally operated in a "mirror" field shape in the Gas Arc Facility; however, operation of the arc so that it extended into only one of the magnetic mirrors gave a reduction in the average probe ion current by more than two orders of magnitude. The character of the probe current also changed from flute dominated to direct current dominated. The most rapid change with anode position occurred when the anode face passed the midplane of the mirror field; a 3-in. (13%) reduction in arc length reduced the probe current by an order of magnitude (at the extreme anode positions the probe current changed about a factor of 2 for a 6-in. displacement). The arc voltage gradually shifted, but only by less than 10% during a reduction in arc length from 39 in. to 15 in. in a 150-amp arc with constant gas flow through the anode. This experiment demonstrated that flute instabilities could be minimized when the shape of the magnetic field satisfied the "minimum B" conditions radially away from the axis.

Research continued on the proposed model for explaining the origin of the hot ions (~500 ev) in energetic carbon arcs. The model (see ORNL-3652, pp. 74-77) incorporates the concepts of energy pumping, inverted level populations, ionic "fusion" collisions, and Coulomb barrier problems such that once the chain of events is initiated, the energy of the ions is believed to escalate to an equilibrium value determined by the mean residence time of ions in the arc, the relative ion population, and the following propagation steps (neglecting power feed and radiative cooling):



The controlled feed of methane gas (CH_4) to a low-pressure, magnetically confined, 14-ft-long hydrogen arc having all-metal electrodes gave carbon ion temperatures which increased monotonically up to 3×10^6 deg K (~ 300 ev) with the intensity of C^{2+} radiation ($\lambda = 4647 \text{ \AA}$), in qualitative agreement with expectations.

A 132-in.-long hydrogen arc, operated in the Long Solenoid Facility at 80 amp and 180 v, has been studied by use of a Langmuir probe and a gridded probe; the e-fold distance was measured to be 0.62 cm at a field strength of 8.25 kilogauss. Axial diffusion of ions has also been measured as a function of magnetic field strength; preliminary results yield a straight line on semilogarithmic paper with the diffusion current decreasing with increasing magnetic field strength (i.e., $I_d \propto \text{KB}^{-m}$).

Ion energies in normal hydrogen arcs operated in the Long Solenoid Facility continued to be low (a few electron volts). The spectral lines of impurity ions exhibit the characteristic Doppler "slant" line effects due to azimuthal drift of ions about the arc column; weak slant line effects which appear superimposed on the neutral hydrogen lines are apparently due to H^+ recombination-type transitions and/or H_2^+ dissociative-excitation processes. A change of magnetic field by a factor of 2 did not affect the overall slant except that for the higher field additional slants at intermediate radii appeared, characteristic of a cylindrical shell of small radius in the arc column.

Experimental Plasma Physics. - We have completed the mathematical analysis of the momentum probe (ORNL-3663, p. 34). This probe measures the momentum distribution of charged particles in a plasma by means of a very simple magnetic analysis principle. The current to the probe wire as a function of magnetic field apparently cannot be expressed in terms of elementary functions; so the basic equations have been expressed in a form suitable for digital computer, and numerical calculations are in progress.

Magnetics and Superconductivity. - An extensive study has been made on how to produce axisymmetrical magnetic fields of great homogeneity with minimum power. This is achieved by finding optimum current-density distributions for the pancake coils of the magnet system. A 7-Mw, 13-in.-I.D. coil has been designed which will produce a field of 60 kilogauss of excellent homogeneity.

Field studies have been made for a hypothetical application of a quadrupole field to DCX-1. Detailed studies about the optimum shape of Ioffe bars gave results which are in good agreement with Luc's calculations for DECA (EUR-CEA-FC-168).

Developmental work on magnetic field microprobes using thin bismuth films is progressing satisfactorily. Experiments with superconducting coils in external magnetic fields can be qualitatively understood by application of the flux-creep theory of Kim et al.

Vacuum Studies for Fusion. - A more detailed analysis was carried out on mass spectra obtained earlier of gases produced by electron bombardment of a surface contaminated with dioctyl phthalate. The compounds formed are believed to be hydrogen, ethylene, butyraldehyde, methane, ethane, and butene, with some water and carbon oxides as possible additional products. There is some evidence that some six- and eight-carbon-

atom molecules were produced, but identification was not possible with the existing data. Decreasing surface temperatures appeared to prevent ready desorption of the products, with only hydrogen being detected at temperatures below 100°K. Increase of surface temperature was accompanied by slight decreases in gas yield up to about 200°C, and no products were detectable at a temperature of 250°C. Filament pyrolysis yielded primarily hydrogen and carbon monoxide (over 95% of the product).

An apparent discrepancy between measured and literature values of the hydrogen compression ratios for diffusion pumps (more than 10^4 and less than 10^3 respectively) has been resolved by calculation of relative oil throughputs for the two cases as based on manufacturer's information. A ratio of about 10^6 was calculated, which is in agreement with the ratio as measured.

Bayard-Alpert ionization gage errors caused by magnetic fields of less than 50 gauss were measured. The greatest error (for the field normal to the collector-filament plane) was 2.5% at 1 gauss and 10% at 2.4 gauss. A minimum error was found for the field orientation parallel to the collector-filament plane and normal to the collector; it did not exceed 1% at fields less than 2 gauss.

BIOLOGY AND MEDICINE

TERRESTRIAL AND FRESH-WATER ECOLOGY

Radiation Effects on Native Mammals: The Effects of *Cuterebra angustifrons* on the Plasma Proteins of *Peromyscus leucopus*. — In 1963 plasma electrophoretic studies on a *Peromyscus leucopus* (white-footed mouse) population at the ORNL reservation indicated a significant reduction in the albumin-globulin ratio (A/G) for those animals infested with larvae of a botfly, *Cuterebra angustifrons*. This condition of skin myiasis was studied more extensively in the summer of 1964. Study of the plasma protein distribution of *P. leucopus* revealed marked alterations for those animals infested with botfly larvae. Reductions in the A/G ratio of animals infested with botfly larvae were correlated significantly to the number of larvae per host. Development of *Cuterebra* larvae in the host was accompanied by progressive depression in the A/G. Correspondingly, recovery in the A/G to the normal values occurred within eight days following loss of the bot. Ingestion of albumin by the bot was proposed as a partial explanation for the reduction in A/G in this type of dipteran parasitosis.

Environmental Radiation Botany: Effects of Soil Moisture on Survival of Gamma-Irradiated Pine Seedlings. — Potted seedlings of *Pinus virginiana* Mill. (scrub pine) received acute ^{60}Co gamma doses of 388, 562, and 900 rads to their apexes. These plants and controls were maintained under constant environmental conditions in a plant growth chamber. Soil moisture levels, however, were varied, with pots receiving no water, 150

ml/week (50 ml thrice weekly), and 450 ml/week (150 ml thrice weekly). During the study, apical needle moisture content was determined [(wet weight - dry weight/dry weight) × 100] until it dropped below 65%, a point below which no seedlings will survive despite additional watering. Plants in all dose groups and controls reached this needle moisture level in 19 to 21 days in the "no water" group, and no significant difference was found between radiation treatments. In the groups receiving 150 ml/week, plants in the 562- and 900-rad treatments required 55 to 64 days to reach the 65% end point, while those in the 388-rad and control groups required only 49 to 52 days. Plants in the higher-dose groups may have required less water due to physiological impairments, therefore surviving this moisture stress for a longer period. In the groups receiving 450 ml/week (adequate moisture), the controls and the 388-rad group maintained relatively constant needle moisture while those in the 562- and 900-rad groups showed a linear decrease in moisture content with time at the rate of 0.6 to 1.0%/day, respectively, for 60 days. This study is still in progress, and no plants maintained at the 450-ml/week moisture level have yet reached the 65% end point. If present trends continue, however, the 388- and 900-rad groups will reach this point in about four months after irradiation, while the low-dose and control groups will still survive.

Evaluation of Fission Product Distribution and Movement in White Oak Drainage System. - The unique "freezing" method has been used to obtain core samples from the bottom of abandoned waste pit No. 2. This method, which utilizes diesel fuel cooled with dry ice as a drilling medium, allows essentially 100% core recovery of the alternating hard and soft shale sequence at the bottom of the pit which cannot be cored satisfactorily with conventional drilling equipment. Radiation measurements of the recovered cores made with a portable ionization-chamber-type instrument, "cutie pie," show maximum dose rates of 8 rads/hr at contact.

RADIOLOGICAL PHYSICS, HEALTH PHYSICS, AND RADIATION INSTRUMENTATION

Radiation Physics and Dosimetry: An Application of the Generalized Concept of Dosimetry to Space Radiations. - A code has been written to determine the distribution of energy losses of an isotropic flux of monoenergetic protons in an array of silicon detectors consisting of a main crystal of dimensions 1 × 1 × 1 cm bounded on each of its six faces by a crystal of dimensions 0.1 × 1 × 1 cm. The code has been used to plot the distribution of energy losses for several selected energies up to 400 Mev.

An energy loss operator is defined which transforms an energy loss distribution function into a dose function. This operator can be used to calculate the dose in rems accurately at the above selected energies and to within a given tolerance at intermediate energies.

An electronic circuit is described which selects energy loss signals from the detector and routes them to the appropriate section of a data processor, thus permitting the calculation of the dose in rems received from an arbitrary flux of high-energy protons.

Radiation Physics and Dosimetry: The Application of Shell Corrections in Stopping Power to Theoretical Dose Studies. - The theoretical evaluation of absorbed radiation dose in tissue from external sources is based on the absorbed energy and rate of linear energy transfer (LET) calculated from the Bethe stopping-power formula. For the chemical elements in tissue, it is known experimentally that shell corrections to the Bethe formula are needed for incident particle energies in the range 0 to 15 Mev. Techniques for evaluating sum rules have been developed and applied successfully to the evaluation of terms in an expansion for the shell corrections suggested by Fano. Shell correction curves that agree with experimental data for a number of metals, ranging in atomic number from beryllium to lead, have been developed (U. Fano and J. E. Turner, "Contributions to the Theory of Shell Corrections," in Penetration of Charged Particles in Matter, National Academy of Sciences-National Research Council Report No. 1133, to be printed). This theory is being applied to the light elements present in soft tissue.

Internal Dose Estimation: Estimation of a Systemic Body Burden of Plutonium. - Computer codes have been reported previously [Health Phys. 8, 61 (1962); ANL-6637, p. 13] which purport to estimate the intake and systemic body burden of plutonium for an employee on the basis of urinalysis data. The model and code are based on data on the retention and excretion of intravenously administered ^{239}Pu citrate by hospital patients. Autopsy data on one employee who worked with ^{239}Pu at intervals during a period of about 11 years have been analyzed by the code in an attempt to determine the extent to which the data agree with the metabolic model used in ICRP Publication 2 to calculate maximum permissible concentrations (MPC) for this radionuclide. It is possible to match the body burden as estimated by autopsy and by the computer code quite closely. However, the fractions of ^{239}Pu depositing in bone and in liver must be assumed to be nearly equal, and a rather short elimination half-time in lung (about 30 days) also must be assumed.

A second attempt to check the accuracy of currently available computer codes for estimation of systemic body burden of ^{239}Pu was undertaken using data on dogs exposed intravenously and by inhalation [Health Phys. 8, 639 (1962)]. The data on retention and excretion following intravenous injection of ^{239}Pu nitrate (0.14 N HNO_3) into dogs were used to establish the metabolic model for the code, as has been done in the case of the human data. Having established the model, the excretion data on dogs exposed to the same material via inhalation were analyzed by the computer to estimate the intake to blood. The estimates by the computer generally agreed to within a factor of 2 with the estimates by the experimenters.

NUCLEAR ENERGY CIVIL EFFECTS

Dosimetry and Spectrometry Research. - A compact, portable decade scaler was built for use in measuring background gamma-ray doses in the areas surrounding the HPRR facility. The scaler is 6 in. high, 9 in. wide, and 5 in. deep. It is operated from rechargeable batteries which have

sufficient energy to operate the scaler continuously for 20 hr. The built-in timer is adjustable from 10 sec to 10 min. An internal regulated high-voltage supply will supply up to 100 μ a of current over a voltage range of 200 to 1500 v. The scaler has a built-in discriminator which is variable from -5 to +5 v. Readout of the lowest three decades is by a special indicator device with additional count storage provided by a four-digit mechanical register. Pulse-pair resolving time is 7 μ sec with the maximum input pulse repetition rate limited to 3000 counts/sec by the mechanical register.

An internal 200 counts/sec test pulse is available for circuit checkout.

ISOTOPE DEVELOPMENT

Stable Isotopes Development. -- Modification of the ion exit slit which forms the positive member (35 kv) of the calutron electrode system has produced improvement in the control of angular divergence of extracted Ar^+ beams. The new slit has two sections or faces which produce the same geometric effect as two slits of different apertures operating at the same potential and separated by a distance of 0.125 in. The face of the slit which has the smaller aperture (0.090 in.) is placed in the conventional position and is nearer the arc; the second face (aperture, 0.185 to 0.25 in.) is oriented toward the negative electrode. Ions formed in the arc chamber are thought to be free to migrate into the auxiliary chamber, which exists between the two faces, prior to being subjected to extraction fields. The presence of this "field-free" region between the arc ribbon and the extraction potential appears to provide a wider range of choice in both arc conditions and extraction fields. By proper adjustment of these two operating parameters, beams of improved focal quality can be achieved from normal output levels (about 60 ma for argon) down to about 2 ma.

Fringing magnetic fields near the front of the calutron tanks are being measured to determine the feasibility of using existing calutron magnets as analyzing fields for inhomogeneous field sector separators. If this approach is practical, standby calutrons could be economically converted into sector-type instruments having a high degree of versatility. Ion outputs from these sector instruments would be lower than those achieved in the calutron; however, the accessibility of the ion source and receiver (outside the main magnetic volume) and the increased mass dispersion possible with an inhomogeneity of 0.8 (greater by factor of 5 over the calutron) outweigh the loss in output expected, particularly for second-pass or radioisotope applications.

Field values measured to date indicate that a stray field of appreciable level exists several feet from the coil periphery. Modification of the calutron into a sector instrument under these conditions requires development of methods to either "cut off" these fields or program them to determine their effect on ion orbits. Once these orbital effects are known, appropriate magnetic shims can be constructed which will compensate for aberrations produced by the stray fields. Both approaches to the problem are being considered.

Special Separations. - An estimated 46 g of enriched ^{240}Pu has been collected in the current plutonium series. This series will be terminated when the requested total of 50 g is reached in order to allow other priority separations to be performed in the contained area. Tentative plans are being made to modify four of the eight calutrons in the containment facility to accommodate equipment necessary to convert these units into 255° inhomogeneous-field separators.

A total of 178 g of the ^{233}U recycle feed material has been purified. The plutonium in this ^{233}U material, which resulted from processing in common equipment, has been reduced from 1.5% to 0.038% using Permutit SK anion resin. Calculations are being made to determine whether this level of plutonium content will interfere with the experiments scheduled to use the ^{233}U material.

Recovery of ^{238}U recycle material was completed, and final results show that 3.2% of the original 10,871 g of feed material was lost to the system.

Target Preparation. - Both supported and self-supported antimony films, free of pinholes, were prepared by evaporation from an electron bombardment heat source. An evaporated NaCl coating on chromium-plated stainless steel was used as the parting agent for the self-supported films; thicknesses of 1 mg/cm^2 or less were obtained.

Considerable improvement in the neutron-generating characteristics of tritium-containing targets was achieved using erbium metal as the sorption medium. By use of a 1-ma current of deuterium ions at an energy of 150 keV, neutrons were generated at the rate of 1×10^{11} neutrons/sec as compared with the previously attained 7×10^{10} neutrons/sec. Another important characteristic of these erbium-tritium targets is the relatively long period (0.75 hr) required for reduction in neutron output by a factor of 2 while under bombardment by deuterium ions.

Radioisotope Research and Development. - One objective of the Source Safety Testing Program is to define a radioisotope source classification system based on the ability of a source capsule to maintain containment of radioactive material under the conditions of its use. Based on a survey of environmental conditions under which sources are currently used and on the testing of more than 400 sources, a source classification system has been developed in which a source can be classified according to its ability to withstand mechanical and temperature-induced stresses. Following issuance of the first draft of the source classification system and receipt of comments from the AEC, the American Standards Association, and industry, a second draft was issued for comment. General testing and classification of commercially available radioisotope sources are continuing, and specific tests on certain sources are performed as requested by the Division of Licensing and Regulation, USAEC.

The Marquardt Corporation has developed a space propulsion device, designated by the trade name "Thruster," in which the propulsive force is supplied by a stream of hydrogen heated by the radioactive decay heat from ^{60}Co . The cooperative test of the Thruster by ORNL and Marquardt utilizing 50,000 curies of ^{60}Co was completed, and Marquardt personnel are proceeding with correlation of the experimental data.

A cooperative program with the Radio Corporation of America will involve the test of a high-temperature thermoelectric device developed by them and fueled with a $^{90}\text{SrTiO}_3$ isotopic power source fabricated by ORNL. Fabrication of the 526-w heat source was completed, using the largest $^{90}\text{SrTiO}_3$ pellets (3.5 in. diam) made to date.

Computer program ISOTOPEs was developed to calculate the optimum time of neutron irradiation for maximum yield, the specific activity of a product isotope in curies per gram of target material, and the combined specific activity of the target and product isotopes for any general first-order reaction or decay problem. The program was written in FORTRAN-62 language for the CDC 1604-A computer.

Program ISOCRUNCH was developed for the IBM 7090 computer by adding optional programs to the basic CRUNCH code and modifying the input and output data formats. ISOCRUNCH can be used to compute the amount of each isotope in a reaction and decay chain for any specified neutron flux and time, to sum the contributions of various chains to the same isotope, to plot the yield of an isotope vs time for a given flux, and to find the optimum time for maximum yield of an isotope in a chain.

Penetration studies of 23-Mev protons from the ORNL 86-Inch Cyclotron into flat-plate target foils were made with the following results:

Foil	Reaction	Thickness Required for >95% of the Total Product Activity (mils)
Platinum	$^{196}\text{Pt}(p,n)^{196}\text{Au}$	2.5
Silver	$^{109}\text{Ag}(p,n)^{109}\text{Cd}$	~5.0
Lead	$^{207}\text{Pb}(p,n)^{207}\text{Bi} +$ $^{208}\text{Pb}(p,2n)^{207}\text{Bi}$	3.5
Manganese	$^{55}\text{Mn}(p,pn)^{54}\text{Mn}$	2.0
Nickel	$^{58}\text{Ni}(p,pn + p,2n)^{57}\text{Ni}$	<2.0
Nickel	$^{58}\text{Ni}(p,\alpha)^{55}\text{Co}$	3.2

These results confirm and amplify the data obtained in earlier studies which showed that in a (p,n) reaction more than 95% of the product is produced in the first 6 mils, in a (p, α) reaction more than 95% of the product is produced in the first 3.2 mils, and in (p,2n) and (p,pn) reactions more than 95% of the product is produced in the first 2 to 3 mils.

OPEN LITERATURE PUBLICATIONS

- Alexeff, Igor, and R. V. Neidigh, "Observation of Burnout in a Steady-State Plasma," *Phys. Rev. Letters* 13, 179 (1964).
- Arakawa, E. T., N. O. Davis, and R. D. Birkhoff, "The Temperature and Thickness Dependence of Transition Radiation from Thin Silver Foils," *Phys. Rev.* 135, A224 (1964).
- Aveston, J., "Hydrolysis of Tungsten(VI): Ultracentrifugation, Acidity Measurements, and Raman Spectra of Polytungstates," *Inorg. Chem.* 3, 981 (1964).
- Aveston, J., and J. S. Johnson, "Hydrolysis of Tantalum(V): Equilibrium Ultracentrifugation and Raman Spectra of Potassium Tantalate," *Inorg. Chem.* 3, 1051 (1964).
- Borie, B., and C. J. Sparks, Jr., "The Short Range Structure of Copper-16 at. % Aluminum," *Acta Cryst.* 17, 827 (1964).
- Burns, J. F., "Auto-Ionization and the Ionization Efficiency Curves for Krypton and Xenon," in Proceedings Third International Conference on Physics of Electronic and Atomic Collisions (London, July 1963), ed. by M. R. C. McDowell, Interscience, New York, 1964.
- Carter, J. G., R. D. Birkhoff, and D. R. Nelson, "Importance of Thermal Equilibrium in Thermoluminescence Measurements," *Health Phys.* 10, 539 (1964).
- Finch, C. B., L. A. Harris, and G. W. Clark, "The Thorite \rightarrow Huttonite Phase Transformation as Determined by Growth of Synthetic Thorite and Huttonite Single Crystals," *Am. Mineralogist* 49, 782 (1964).
- Folson, T. R., C. Feldman, and T. C. Rains, "Variation of Cesium in the Ocean," *Science* 144, 538 (1964).
- Fox, C. W., and G. M. Slaughter, "Brazing of Ceramics," *Welding J.* 43, 591 (1964).
- Hill, N. A., and O. B. Cavin, "Monoclinic-Cubic Transformation in Thorium Dicarbide," *J. Am. Ceram. Soc.* 47, 360 (1964).
- Koertyohann, S. R., and C. Feldman, "Atomic Absorption Spectroscopy Using Long Absorption Path Lengths and a Demountable Hollow Cathode Lamp," in Proceedings 14th Annual Mid-America Spectroscopy Symposium, Chicago, May 20-23, 1963 (Developments in Applied Spectroscopy, Vol. 3), Plenum Press, New York, 1964.
- Lietzke, M. H., R. W. Stoughton, and Marjorie P. Lietzke, "A Comparison of Several Methods for Inverting Large Symmetric Positive Definite Matrices," *Math. Comp.* 18, 449 (1964).
- Manning, D. L., "Voltammetry of Nickel in Molten Lithium Fluoride-Sodium Fluoride-Potassium Fluoride," *J. Electroanal. Chem.* 7, 302 (1964).
- Melton, C. E., and W. H. Hammill, "Appearance Potentials of Positive and Negative Ions by Mass Spectrometry," *J. Chem. Phys.* 41, 546 (1964).
- Moak, C. D., "Experiments with Heavy Ions," *Nucl. Instr. Methods* 28, 155 (1964).

- Moak, C. D., W. M. Good, R. F. King, J. W. Johnson, H. E. Banta, J. Judish, and W. H. duPreez, "Nanosecond Pulsing for Van de Graaff Accelerators," *Rev. Sci. Instr.* 35, 672 (1964).
- Morton, J. E., H. A. Parker, E. I. Wyatt, and L. T. Corbin, "Shielded Facility for Use in the Analysis of Radioisotopes," in Proceedings 11th Conference on Hot Laboratories and Equipment (New York, 1963), American Nuclear Society, Hinsdale, Illinois, 1963.
- Nelson, D. J., "Deposition of Strontium in Relation to Morphology of Clam (Unionidae) Shells," *Verhandl. Intern. Verein Limnol.* 15, 893 (1964).
- Nelson, D. J., and C. W. Wiser, "Uptake and Elimination of Cobalt-60 by Crayfish," *Am. Midland Naturalist* 72, 181 (1964).
- Oen, O. S., and M. T. Robinson, "Monte Carlo Range Calculations for a Thomas-Fermi Potential," *J. Appl. Phys.* 35, 2515 (1964).
- Pal, B. C., and C. A. Horton, "The Structure of 3-Methyladenine, and Methylation of 6-Dimethylaminopurine," *J. Chem. Soc.* 1964, 400.
- Reynolds, S. A., "Choosing Optimum Counting Methods and Radiotracers," *Nucleonics* 22(8), 104 (1964).
- Ricci, E., "Nomographs for Calculating Induced Radioactivity and Decay," *Nucleonics* 22(8), 105 (1964).
- Ritchie, R. H., J. C. Ashley, and L. C. Emerson, "Optical Bremsstrahlung and Transition Radiation from Irradiated Media," *Phys. Rev.* 135, A759 (1964).
- Ross, H. H., "Liquid Scintillation Counting of Carbon-14 Using a Balanced Quenching Technique," *Intern. J. Appl. Radiation Isotopes* 15, 273 (1964).
- Sakai, M., and T. Tamura, "Inelastic Scattering of Protons by Cd^{114} and Possible Quadrupole-Octupole Two-Phonon States," *Phys. Letters* 10, 323 (1964).
- Schmitt, H. W., and N. Feather, "Interpretation of the Fragment Mass Distribution for U^{235} Thermal-Neutron-Induced Fission with Long-Range Alpha Emission," *Phys. Rev.* 134, B565 (1964).
- Shaffer, J. H., W. R. Grimes, G. M. Watson, D. R. Cuneo, J. E. Strain, and M. J. Kelley, "The Recovery of Protactinium and Uranium from Molten Fluoride Systems by Precipitation as Oxides," *Nucl. Sci. Eng.* 18, 177 (1964).
- Snyder, W. S., "The LET Distribution of Dose in Some Tissue Cylinders," in Biological Effects of Neutron and Proton Irradiations, IAEA, Vienna, 1964.
- Stockdale, J. A., and G. S. Hurst, "Swarm Measurement of Cross Sections for Dissociative Electron Capture in Heavy Water, Chlorobenzene, and Bromobenzene," *J. Chem. Phys.* 41, 255 (1964).
- Stockdale, J. A., G. S. Hurst, and L. G. Christophorou, "Capture of Low Energy Electrons in Chlorobenzene and Bromobenzene," *Nature* 202, 459 (1964).

- Wagner, R., P. D. Miller, T. Tamura, and H. Marshak, "The Interaction of 350-kev Polarized Neutrons with Oriented ^{165}Ho Nuclei," Phys. Letters 10, 316 (1964).
- Walton, Derek, "Phonon Scattering by the F-Center Electron," Phys. Rev. 135, A753 (1964).
- Watson, C. D., and W. W. Parkinson, "Irradiation of Bituminous Materials," chap. 6 in Bituminous Materials, vol. I, ed. by A. J. Hoiberg, Interscience, New York, 1964.
- Weekley, R. E., and J. A. Norris, "A Versatile Electronic Computer for Photoelectric Spectrochemical Analysis," Appl. Spectry. 18(1), 21 (1964).
- Young, J. P., and G. P. Smith, "Coordination of Fluoride Ions About Nickel(II) Ions in the Molten LiF-NaF-KF Eutectic," J. Chem. Phys. 40, 913 (1964).

FOREIGN VISITORS

<u>Name</u>	<u>Affiliation</u>	<u>Citizen of</u>
Accary, A. R.	French CEA	France
Ando, T.	Ishikawajima-Harima Heavy Industries Co.	Japan
Asai, H.	Japanese Study Team	Japan
Anselin, F. L. G.	French CEA	France
Aung, H.	University of Tennessee	Burma
Aymar, R. J.	French CEA	France
Benavides, J.	National Legislative Assembly	Costa Rica
Brechna, H.	Stanford University	Switzerland
Clark, C. D.	Reading University	Great Britain
Costa, P. I.	French CEA	France
Dirian, J. M.	French CEA	France
Dostrovsky, I.	Brookhaven National Laboratory	Israel
Doucet, H. J.	Laboratoire de Physique des Milieux Ionises	France
Edge, R. D.	Yale University	Great Britain
Engeli, M.	Federal Institute of Technology	Switzerland
Guardia, C. M.	National Legislative Assembly	Costa Rica
Halsall, M. J.	Atomic Energy of Canada Limited	Great Britain
Iizuka, T.	Hitachi, Limited	Japan
Ikegami, H.	Tokyo Institute of Technology	Japan
Inoue, K.	Japanese Study Team	Japan
Kadoya, S.	Japanese Study Team	Japan
Kato, M.	University of Tokyo	Japan
Kitade, K.	Japanese Study Team	Japan
Komeno, A.	Japanese Study Team	Japan
Kozeki, M.	Japanese Study Team	Japan

<u>Name</u>	<u>Affiliation</u>	<u>Citizen of</u>
Lindstrom-Lang, C. U.	AEC, Denmark	Denmark
Lomer, J.	University of Reading	Great Britain
Maki, H.	Hitachi Research Laboratory	Japan
Maruta, Y.	Kao Soap Company	Japan
Mermagen, J.	Cambridge University	Great Britain
Morgan, W.	Fisk University	Jamaica
Nagahata, Y.	Japanese Study Team	Japan
Noma, I.	Japanese Study Team	Japan
Omori, N.	Japanese Study Team	Japan
Pascard R.	French CEA	France
Petit, A.	French CEA	France
Remarque, J. F.	American Elsevier Publishing Co.	Netherlands
Rivas, D.	Self - Interpreter	Cuba
Ruland, W.	European Research Associates	Germany
Runnals, O. J. C.	Atomic Energy of Canada Limited	Canada
Sarantites, D. G.	Washington University	Greece
Schueler, W. A.	Oak Ridge Technical Enterprises Corp.	Austria
Sennis, C.	CNEN, Italy	Italy
Silberman, E.	Argentine AEC	Argentina
Skillicorn, B.	High Voltage Engineering Corporation	Great Britain
Stammreich, H.	University of Sao Paulo	Brazil
Ting, S. F.	University of Tennessee	China
Viquez, E.	National Legislative Assembly	Costa Rica
Viquez, E., Jr.	Self	Costa Rica
Williams, J. E.	Culham Laboratory	Great Britain
Woodrow, J.	United Kingdom AEA	Great Britain
Yamada, T.	Nagoya Institute of Technology	Japan
Yamaguchi, H.	Japanese Study Team	Japan
Yamamoto, M.	Japanese Study Team	Japan
Yoshida, S.	University of Osaka	Japan
Yoshikawa, Y.	Japanese Study Team	Japan

Reports issued in this series during the past year:

August 1963	ORNL-3508
September 1963	ORNL-3517
October 1963	ORNL-3532
November 1963	ORNL-3543
December 1963	ORNL-3561
January 1964	ORNL-3568
February 1964	ORNL-3590
March 1964	ORNL-3614
April 1964	ORNL-3628
May 1964	ORNL-3647
June 1964	ORNL-3663
July 1964	ORNL-3680



ORNL-3701
C-44a - Nuclear Technology - Materials
M-3679 (35th ed.)

INTERNAL DISTRIBUTION

- | | |
|--------------------------|---------------------------------|
| 1. I. Alexeff | 50. W. F. Gauster |
| 2. C. F. Baes | 51. J. H. Gillette |
| 3. E. A. Bagley | 52. W. Y. Gissel |
| 4. P. S. Baker | 53. H. E. Goeller |
| 5. C. R. Baldock | 54. C. D. Goodman |
| 6. L. H. Barker | 55. A. T. Gresky |
| 7. S. E. Beall | 56. J. C. Griess |
| 8. E. E. Beauchamp | 57. W. R. Grimes |
| 9. P. R. Bell | 58. P. A. Haas |
| 10. D. S. Billington | 59. C. S. Harrill |
| 11. C. A. Blake | 60. J. C. Hart |
| 12. R. E. Blanco | 61. P. N. Haubenreich |
| 13. F. F. Blankenship | 62. M. R. Hill |
| 14. E. P. Blizard | 63. C. J. Hochanadel |
| 15. J. O. Blomeke | 64. A. Hollaender |
| 16. A. L. Boch | 65. L. B. Holland |
| 17. E. G. Bohlmann | 66. R. W. Horton |
| 18. C. J. Borkowski | 67. F. T. Howard |
| 19. G. E. Boyd | 68. A. S. Householder |
| 20. M. A. Bredig | 69. H. H. Hubbell |
| 21. J. C. Bresee | 70. G. S. Hurst |
| 22. R. B. Briggs | 71. K. E. Jamison |
| 23. R. E. Brooksbank | 72. G. H. Jenks |
| 24. K. B. Brown | 73. R. W. Johnson |
| 25. F. R. Bruce | 74. R. J. Jones |
| 26. W. D. Burch | 75. W. H. Jordan |
| 27. T. H. J. Burnett | 76. P. R. Kasten |
| 28. A. D. Callihan | 77. G. W. Keilholtz |
| 29. A. E. Cameron | 78. G. G. Kelley |
| 30. T. E. Cole | 79. M. T. Kelley |
| 31. C. F. Coleman | 80. E. M. King |
| 32. E. L. Compere | 81. K. A. Kraus |
| 33. D. D. Cowen | 82. Laboratory Shift Supervisor |
| 34. J. A. Cox | 83. J. A. Lane |
| 35. F. L. Culler | 84. D. M. Lang (K-25) |
| 36. J. E. Cunningham | 85. C. E. Larson |
| 37. R. A. Dandl | 86. C. F. Leitten, Jr. |
| 38. Wallace Davis | 87. R. E. Leuze |
| 39. J. S. Drury | 88. L. F. Lieber |
| 40. J. L. Dunlap | 89. T. A. Lincoln |
| 41. A. C. England | 90. S. C. Lind |
| 42. M. F. Fair | 91. R. B. Lindauer |
| 43. D. E. Ferguson | 92. R. S. Livingston |
| 44-47. J. L. Fowler | 93. J. T. Long |
| 48. J. H. Frye, Jr. | 94. J. E. Longendorfer |
| 49. J. L. Gabbard (K-25) | 95. L. O. Love |

- | | |
|------------------------|--|
| 96. R. N. Lyon | 130. A. H. Snell |
| 97. H. G. MacPherson | 131. W. S. Snyder |
| 98. F. C. Maienschein | 132. W. L. Stirling |
| 99. J. A. Martin | 133. R. W. Stoughton |
| 100. H. F. McDuffie | 134. H. Stringfield |
| 101. J. R. McNally | 135. E. G. Struxness |
| 102. R. A. McNees | 136. J. C. Suddath |
| 103. A. J. Miller | 137. W. H. Sullivan |
| 104. C. E. Miller, Jr. | 138. C. D. Susano |
| 105. E. C. Miller | 139. J. A. Swartout |
| 106. K. Z. Morgan | 140. E. H. Taylor |
| 107. W. L. Morgan | 141. R. E. Thoma |
| 108. E. J. Murphy | 142. C. D. Watson |
| 109. R. V. Neidigh | 143. B. S. Weaver |
| 110. M. L. Nelson | 144. M. S. Wechsler |
| 111. G. W. Parker | 145. A. M. Weinberg |
| 112. R. B. Parker | 146. M. E. Whatley |
| 113. P. Patriarca | 147. J. C. White |
| 114. S. Peterson | 148. E. O. Wollan |
| 115. J. J. Pinajian | 149. R. W. Worsham |
| 116. M. E. Ramsey | 150. R. G. Wymer |
| 117. A. W. Riikola | 151. Gale Young |
| 118. L. P. Riordan | 152. W. Zobel |
| 119. A. F. Rupp | 153. A. Zucker |
| 120. A. D. Ryon | 154-155. Central Research Library |
| 121. H. C. Savage | 156-157. ORNL - Y-12 Technical Library |
| 122. H. W. Savage | Document Reference Section |
| 123. A. W. Savolainen | 158. Reactor Division Library |
| 124. H. E. Seagren | 159. Biology Library |
| 125. C. H. Secoy | 160-313. Laboratory Records Department |
| 126. E. D. Shipley | 314. Laboratory Records, ORNL R.C. |
| 127. O. Sisman | 315. General Engineering and |
| 128. J. R. Sites | Construction Library |
| 129. M. J. Skinner | |

EXTERNAL DISTRIBUTION

- 316. Division of Reactor Development, AEC, Washington (J. M. Simmons)
- 317-326. Research and Development Division, AEC, ORO
- 327. Aeroprojects, Inc. (W. B. Tarpley)
- 328. Allis-Chalmers Manufacturing Co. (W. F. Banks)
- 329-331. Ames Laboratory, Iowa State College (F. H. Spedding)
- 332-334. Argonne National Laboratory (A. V. Crewe)
- 335. Atomics International (H. Pearlman)
- 336. Babcock and Wilcox Co. (Atomic Energy Division)
- 337-338. Battelle Memorial Institute (H. W. Russell)
- 339-341. Brookhaven National Laboratory (M. Goldhaber)
- 342. Bureau of Mines, Salt Lake City (J. B. Clemmer)
- 343-350. General Atomic (General Dynamics Corp.) (Manager)
- 351-352. General Nuclear Engineering Corp. (J. West)
- 353. Kaiser Engineers (P. D. Bush)

- 354-355. Knolls Atomic Power Laboratory (K. R. Van Tassell)
- 356-357. Lawrence Radiation Laboratory (H. Fidler)
- 358-359. Los Alamos Scientific Laboratory (N. E. Bradbury)
- 360-361. National Bureau of Standards (L. S. Taylor)
- 362. Nuclear Metals, Inc. (A. R. Kaufmann)
- 363-364. Philadelphia Electric Co. (L. R. Gaty)
- 365. Phillips Petroleum Company, NRTS (J. P. Lyon)
- 366. Sanderson and Porter (Atomic Energy Division)
- 367. Union Carbide Corporation (R. W. McNamee)
- 368. USAEC, Assistant General Manager (S. G. English)
- 369. USAEC, Division of Biology and Medicine (C. L. Dunham)
- 370-372. USAEC, Division of Isotope Development (P. C. Aebersold)
- 373. USAEC, Division of Production (F. P. Baranowski)
- 374. USAEC, Division of Raw Materials (J. C. Johnson)
- 375-389. USAEC, Division of Reactor Development (F. K. Pittman)
- 390-395. USAEC, Division of Research (P. W. McDaniel)
- 396. USAEC, Division of Research, Special Projects Branch, Washington (Dorothy Smith)
- 397-398. USAEC, Division of Technical Information (Technical Reports Library and 1 copy to R. E. Bowman, Room D-403)
- 399-400. USAEC, Chicago Operations Office
- 401. USAEC, Lockland Aircraft Reactors Operations Office (H. H. Gorman)
- 402-403. USAEC, San Francisco Operations Office (R. Hughey)
- 404-405. USAEC, Savannah River Operations Office (H. Rahner)
- 406. Westinghouse Electric Corp. (A. Squire)
- 407-651. Given distribution as shown in M-3679 (35th ed.) category C-44a and those addresses shown in C-44b, C-44c, and C-44d, which do not receive copies under C-44a